CONTRACT MELiSSA 1993, PRF 130820.

MODELING OF PHYSICAL LIMITATIONS IN PHOTOBIOREACTORS.

APPLICATIONS TO SIMULATION AND CONTROL OF THE *Spirulina* COMPARTMENT OF THE MELiSSA ARTIFICIAL ECOSYSTEM.

TECHNICAL NOTE 19.1.

Laboratoire de Génie Chimique Biologique.
Université Blaise Pascal.
24, avenue des Landais. 63177 AUBIERE CEDEX. FRANCE.

MELiSSA. Contract PRF 130-820.

MODELING OF PHYSICAL LIMITATIONS IN PHOTOBIOREACTORS.

TN.19.1: Adaptation of the light energy transfer model to cylindrical geometries.

CORNET, J-F., DUSSAP C-G., GROS, J-B.
Laboratoire de Génie Chimique Biologique- 63177 AUBIERE.

The study of the coupling between physical limitation by light and growth kinetics in photobioreactors leads to very complex partial differential equations. Modeling of light transfer in photobioreactors require an equation including two parameters for light absorption and scattering in the culture medium. A simple model based on the simplified, monodimensionnal equations of Schuster for radiative transfer has been published for rectangular geometries (A structured model for simulation of cultures of the cyanobacterium *Spirulina platensis* in photobioreactors. Part I and II, see appendix). This approach provides a simple way to determine a working illuminated volume in which growth occurs, therefore allowing identification of coefficients in kinetic models of cultures. These parameters might then be extended to the analysis of more complex geometries such as cylindrical reactors. Moreover, this model allows the behavior of batch or continuous cultures of cyanobacteria under light and mineral limitations to be predicted.

In this technical note, the physical part of the light transfer model already published is adapted to cylindrical geometries. Such a model, including the biological part, provides low calculation time and appears as a good numerical tool to perform the control of the *Spirulina* compartment of MELiSSA.

The background for the comprehension of this technical note is included in the two papers given in appendix and the reader will have first to cross-refer to them.

The nomenclature used is the nomenclature used in the two papers in appendix.

1- New definition of the working illuminated volume in rectangular geometries.

The extension of the model written in rectangular coordinates to more complex geometries requires a more general expression for the working illuminated volume to be defined. In effect, the working illuminated volume has been defined as the volume of the

photoreactor in which growth would be exponential, the other part of the reactor being inactive (paper I in appendix). This working illuminated volume has been experimentally calculated in parallelepipedic photoreactors (Roux flasks) by measuring the maximum biomass concentrations C_{XI} obtained by exponential growth in various incident light and reactor size conditions. This maximum biomass concentration has been determined by extrapolating the curves r_X/μ_M versus C_X for exponential and linear growth phases, the intercept of which giving C_{XI} (fig. 6, paper I).

The different determinations of C_{XI} performed on *S. platensis* cultivated in Roux flasks have indicated that the maximum biomass concentration C_{XI} that could be obtained in exponential growth, always corresponds to a constant limit value of the radiant energy flux leaving the reactor i.e:

$$F_{min} = 1.0 \pm 0.1\ W.m^{-2}$$

Conversely, this value can be used for automatic calculations; to determine, via the light transfer model developed in rectangular coordinates, the maximum biomass concentration obtainable by exponential growth in given incident light conditions. The value of C_{XI} has been then used to calculate the ratio of working illuminated length over total length $L_2 = (C_{XI}/C_X)L$.

At present time, its seems more judicious for extrapolating to other geometries, to directly use the radiant energy profile expression for the determination of the limit thickness above which the radiant flux is less than the limit value of 1 W/m^2 instead of solving the expression given by the transmittance ratio, which cannot be extended to others geometries. The new definition for the working illuminated volume, in rectangular coordinates, comes from the resolution of:

$$2\frac{(1+\alpha)e^{-\delta(Z_2-1)} - (1-\alpha)e^{\delta(Z_2-1)}}{(1+\alpha)^2 e^{\delta} - (1-\alpha)^2 e^{-\delta}} - \frac{F_{min}}{F_0} = 0$$

where $Z_2 = L_2/L$ is the root leading to the working length L_2,
$\delta = [z_a Ea + (1+z_g)Es]\ C_{XA}\alpha L$ (equation 2, paper II),
and $F_{min} = 1$ W/m^2.

After comparison with the experimental results obtained in Roux flasks, this new definition has led to a new value of the parameter μ'_M which is obtained by identification and equal to 0.54 h^{-1} (instead of 0.52 h^{-1}).

2- Monodimensional equations of radiative transfer for cylindrical photobioreactors.

In order to obtain the profiles of radiant energy available into the cylindrical photobioreactor, the probem of radiative transfer has been simplified to a one-dimension problem, from the assumptions of Schuster (paper I in appendix). Assuming that the incident

light energy is radially distributed at the external wall, and neglecting the angular distribution of the incident intensity, the field of radiation is split into two opposite fluxes F_z^+ and F_z^- along the r-axis (figure 1).

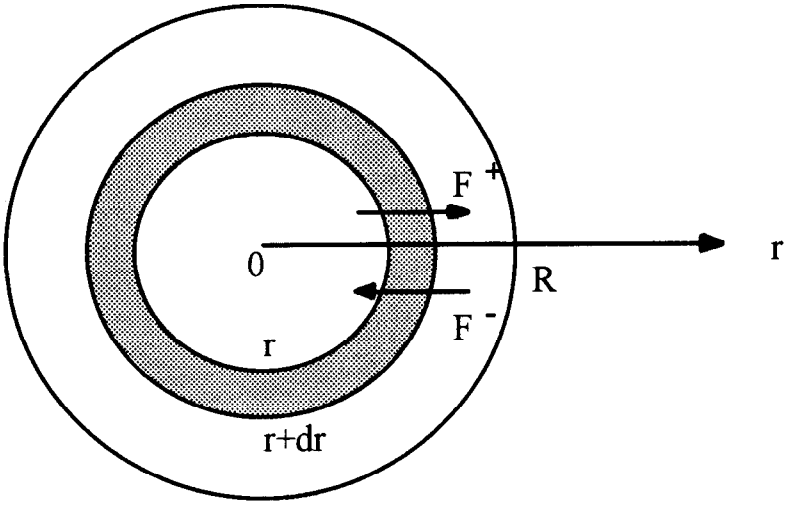

Figure 1: Global radiant energy balances on an elemental volume of thickness dr.

Using the same method as in paper I, the balance of radiant energy flux in cylindrical coordinates leads to establish two energy balances on the elemental volume of thickness dr considered separately for the direct and the reverse fluxes F_z^+ and F_z^-; the following system is thus derived:

$$\begin{cases} \dfrac{1}{r}\dfrac{d(rF_r^+)}{dr} = -EaC_X F_r^+ + \dfrac{1}{2}EsC_X(F_r^- - F_r^+) \\ \dfrac{1}{r}\dfrac{d(rF_r^-)}{dr} = EaC_X F_r^- + \dfrac{1}{2}EsC_X(F_r^- - F_r^+) \end{cases}$$

It must be noticed that the left hand side of the two above equations is the divergence of the radiant energy flux **F** with $\dfrac{\partial F}{\partial \theta} = \dfrac{\partial F}{\partial \phi} = 0$. Therefore, this system of equations has the same form as in the previous paper, but expressing the divergence in cylindrical coordinates.

The system of differential equations can be solved from the appropriate boundary conditions:

$$\begin{cases} r = 0, \ F_r^+ = F_r^- \\ r = R, \ F_r^- = F_R \end{cases}$$

The first equation expresses the fact that the flux is a continuous function on the axis of the cylinder and the second one indicates that the flux inside the reactor at the external wall is determined by the external illuminating device.

With $\delta = C_X\sqrt{Ea(Ea+Es)}$,and $\alpha = \sqrt{\frac{Ea}{Ea+Es}}$, the solutions for the direct and the reverse fluxes are given by:

$$\frac{F_r^-}{F_R} = \frac{R}{r}\frac{\cosh \delta r + \alpha \sinh \delta r}{\cosh \delta R + \alpha \sinh \delta R}$$

$$\frac{F_r^+}{F_R} = \frac{R}{r}\frac{\cosh \delta r - \alpha \sinh \delta r}{\cosh \delta R + \alpha \sinh \delta R}$$

From the definition of the radiant light energy available, we have $4\pi J_r = F_r^+ + F_r^-$, and so:

$$\frac{4\pi J_r}{F_R} = \frac{R}{r}\frac{2\cosh \delta r}{\cosh \delta R + \alpha \sinh \delta R}$$

Remembering that:

$-\nabla . \mathbf{F} = \alpha\delta 4\pi J_r = A = -\frac{1}{r}\frac{d(rF_r)}{dr}$, we obtain finally the normalized flux profile:

$$\frac{F_r}{F_R} = -2\alpha\frac{R}{r}\frac{\sinh \delta r}{\cosh \delta R + \alpha \sinh \delta R}$$

It must be noticed that the conservative case in which $\alpha = 0$ and $\nabla . \mathbf{F} = 0$ implies the produce rF_r to be a constant along the r-axis.

From the new dimensionless variables defined in paper I, Z = r/R, and $\delta = (Ea+Es)\ \alpha\ C_X\ R$, the following expressions for the radiant energy available and the radiant energy flux, are obtained:

$$\frac{4\pi J_r}{F_R} = \frac{1}{Z}\frac{2\cosh \delta Z}{\cosh \delta + \alpha \sinh \delta}$$

$$\frac{F_r}{F_R} = -2\alpha \frac{1}{Z} \frac{\sinh \delta Z}{\cosh \delta + \alpha \sinh \delta}$$

The normalized profiles $4\pi J_r/F_R$ and F_r/F_R along the Z axis are given in figures 2 and 3 for different values of δ as parameter.

In order to obtain the working illuminated volume in cylindrical coordinates, it is necessary to solve the algebraic equation:

$$\frac{1}{Z_2} \frac{2\cosh \delta Z_2}{\cosh \delta + \alpha \sinh \delta} - \frac{F_{min}}{F_R} = 0$$

with F_{min} = 1 W/m^2 as previously stated and $Z_2 = R_2/R$, R_2 being the working illuminated radius.

Special attention should be paid to the fact this equation could present either two roots between [0-R] for high values of δ, or no solution for low values of δ. This last case means that the working volume is identical to the total volume of the reactor.

Let R_2 and R'_2 to be the two roots obtained in the general case (R'_2 is the root near the center of the reactor), thus the mean growth rate is given by (paper II, in appendix):

$$<\mu'> = \frac{1}{\pi R_2'^2} \int_0^{R'^2} 2\pi r \mu'_M \frac{4\pi J_r}{K_J + 4\pi J_r} dr + \frac{1}{\pi (R - R_2)^2} \int_{R_2}^{R} 2\pi r \mu'_M \frac{4\pi J_r}{K_J + 4\pi J_r} dr$$

and the illuminated fraction of the reactor is $\gamma = \frac{R_2'^2}{R^2} + \frac{(R - R_2)^2}{R^2}$.

The first terms of the right hand sides of these two equations are often negligible because R'_2 is very low if δ is high enough.

It must be noticed that the equation (40) in paper I provides an approximation of γ in cylindrical coordinates with an accuracy less than 5%.

From the notations introduced in the second paper, one remember here the values of the main parameters:

$$\alpha = [z_a Ea/(z_a Ea + (1+z_g)Es]^{1/2}$$
$$\delta = [z_a Ea + (1+z_g)Es] C_{XA}\, \alpha\, R$$
$$Ea = 871 \text{ m}^2/\text{kg of antenna}$$
$$Es = 167 \text{ m}^2/\text{kg of total biomass}$$
$$K_J = 20 \text{ W/m}^2$$
$$\mu'_M = 0.54 \text{ h}^{-1}$$

The values of the coefficients Ea and Es are different with regard to paper II because they have been determined here by a more accurate method. The new definitions of α and δ take into account te subdivision of the biomass in different compartments in paper II. Moreover, δ has been converted in dimensionless form.

3- Obtention of the flux F_R at the boundary with an integrating sphere photometer.

It may be difficult to obtain an accurate value of the incident flux F_R onto the reactor. This can be made by mean of an integrating sphere photometer placed at the center of the reactor (r = 0). In this case, if E_b is the total radiant energy absorbed by the sphere and r_b the radius of the sphere, we have:

$$\frac{E_b}{F_R} = \frac{1}{4\pi r_b^2}\left[\int_0^{\pi} \pi r_b^2 \sin\theta \left(4\pi J_{|r_b \sin\theta}\right) d\theta + \int_{\pi}^{2\pi} \pi r_b^2 \sin\theta \left(4\pi J_{|r_b \sin\theta}\right) d\theta\right]$$

which leads after calculation to:

$$\frac{E_b}{F_R} = \frac{R}{r_b(\cosh\delta R + \alpha \sinh\delta R)} \int_0^{\pi} \cosh(\delta r_b \sin\theta) d\theta$$

Remembering the expression of the first-species modified Bessel function of 0 order I_0, we obtain:

$$\frac{E_b}{F_R} = \frac{R\pi I_0(\delta r_b)}{r_b(\cosh\delta R + \alpha \sinh\delta R)}$$

If $\delta r_b < 1$, i.e. the biomass concentration is lower than 0.4 kg/m^3, the following approximation is valid:

$$\frac{E_b}{F_R} \approx \frac{\pi R}{r_b(\cosh\delta R + \alpha \sinh\delta R)}\left[1 + \frac{(\delta r_b)^2}{4}\right]$$

With the dimensionless variables defined above $Z_b = r_b/R$ and $\delta = (Ea+Es)\ \alpha\ C_X\ R$, the equations giving Eb/Fr should be obtained from:

$$\frac{E_b}{F_R} = \frac{1}{Z_b} \frac{1}{(\cosh\delta R + \alpha \sinh\delta R)}\left[\int_0^{\pi} \cosh(\delta Z_b \sin\theta) d\theta\right]$$

These equations allow to determine the exact value of the mean incident flux F_R by some measurements at low concentrations of biomass in the reactor or no biomass ($\alpha = 0$).

4- Equations for the model.

The table III of the second published paper (paper II in appendix) is then adapted as follows for cylindrical reactors:

$4\pi J_r$ calculation:

$$\frac{4\pi J_r}{F_R} = \frac{1}{Z}\frac{2\cosh\delta Z}{\cosh\delta + \alpha\sinh\delta}$$

$$\alpha = \left[z_a Ea \Big/ \left(z_a Ea + \left(1+z_g\right)Es\right)\right]^{\frac{1}{2}}$$

$$\delta = \left[z_a Ea + \left(1+z_g\right)Es\right]C_{XA}\alpha R$$

Working illuminated radius R_2 calculation:

$$\frac{1}{Z_2}\frac{2\cosh\delta Z_2}{\cosh\delta + \alpha\sinh\delta} - \frac{F_{min}}{F_R} = 0$$

$$Z_2 = \frac{R_2}{R}$$

$$F_{min} = 1 W/m^2$$

Average of specific growth rates:

$$< R > = < \mu' > \gamma C_{PC}$$

$$< \mu' > = \frac{1}{\pi R_2'^2}\int_0^{R'^2} 2\pi r \mu'_M \frac{4\pi J_r}{K_J + 4\pi J_r} dr + \frac{1}{\pi(R-R_2)^2}\int_{R_2}^{R} 2\pi r \mu'_M \frac{4\pi J_r}{K_J + 4\pi J_r} dr$$

$$<\mu'>\approx \frac{1}{\pi(R-R_2)^2}\int_{R_2}^{R} 2\pi r\mu'_M \frac{4\pi J_r}{K_J+4\pi J_r}dr$$

or directly $$<R>\approx C_{PC}\frac{2\mu'_M}{R^2}\int_{R_2}^{R} r\frac{4\pi J_r}{K_J+4\pi J_r}dr$$

Kinetic equations:

$$<r_{XA}>=<R>\frac{C_N}{K_N+C_N}\frac{C_S}{K_S+C_S}$$

$$<r_{CH}>=z_{CH}<r_{XA}>$$

$$<r_{PC}>=z_{PC}<R>\left[\frac{C_N}{K_N+C_N}\frac{C_S}{K_S+C_S}-\left(\frac{K_N}{K_N+C_N}+\frac{K_S}{K_S+C_S}\right)\right]$$

$$<r_P>=z_P<R>\left[\frac{C_N}{K_N+C_N}\frac{C_S}{K_S+C_S}-q\frac{K_S}{K_S+C_S}\right]$$

$$<r_N>=-Y_{N/XA}<r_{XA}>$$

$$<r_S>=-Y_{S/XA}<r_{XA}>$$

$$<r_{XT}>=<R>\left[\frac{C_N}{K_N+C_N}\frac{C_S}{K_S+C_S}+\frac{C_{PC}}{K_{PC}+C_{PC}^2}\left(\frac{K_N}{K_N+C_N}+\frac{K_S}{K_S+C_S}\right)\right]$$

Conclusions.

The simplified, monodimensional model of radiative transfer based on the asumptions of Schuster and established for rectangular geometries has been extended in this technical note to cylindrical geometries. This new physical model requires the photobioreactor to be radially and homogeneously illuminated to be applicable. This experimental condition being difficult to realize, an equation has been developed in order to obtain the mean value of the radiant energy flux at the boundary of the reactor from a measurement with an integrating sphere photometer.

The model developed allows to utilize the kinetic equations which have been published in the two papers given in appendix with the same kinetic parameters.

The validity of these parameters which have been identified in the range 4-20 W/m^2 will have to be inproved by experimentation for higher incident radiant energy fluxes.

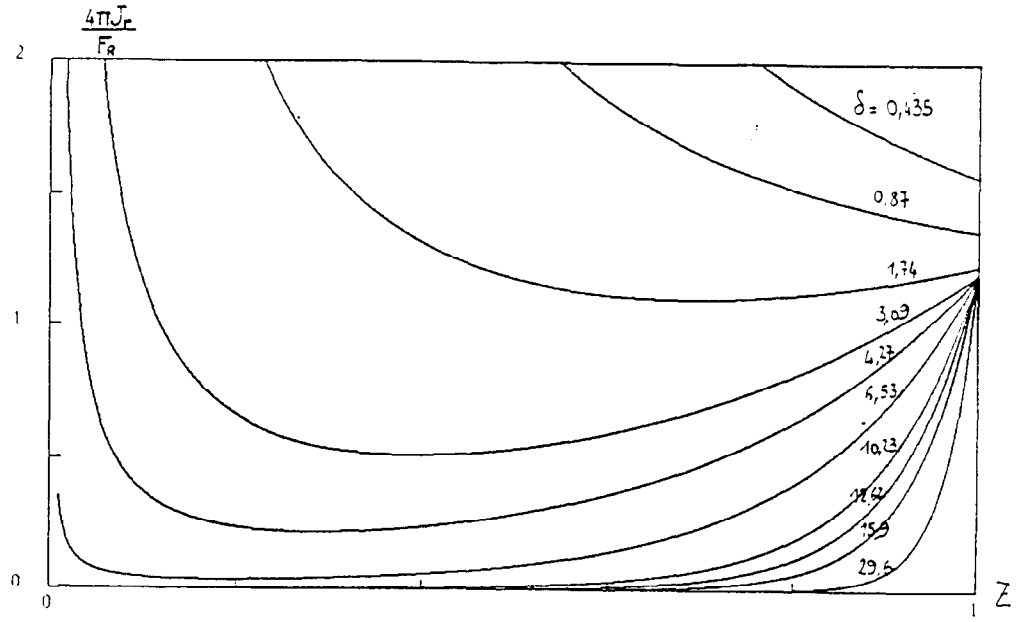

Figure 2: profiles of normalized radiant energy available along the Z axis (δ as parameter).

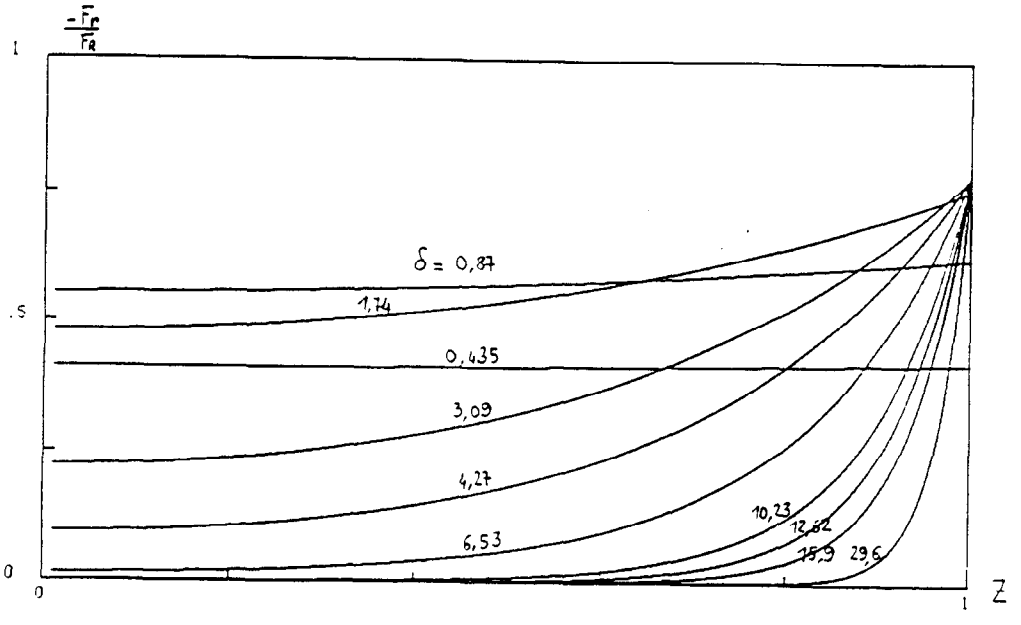

Figure 3: profiles of normalized radiant energy flux along the Z axis (δ as parameter).

APPENDIX

A Structured Model for Simulation of Cultures of the Cyanobacterium *Spirulina platensis* in Photobioreactors: I. Coupling Between Light Transfer and Growth Kinetics

J. F. Cornet
Matra-Espace—Applications de la microgravité, 78146 Vélizy-Villacoublay, France

C. G. Dussap*
Laboratoire de Génie Chimique Biologique, Université Blaise Pascal, Clermont II, 63177 Aubière, Cédex, France

G. Dubertret
Laboratoire de Biochimie Fonctionnelle des Membranes Végétales, C.N.R.S, 91198 Gif-sur-Yvette, Cédex, France

Received August 29, 1991/Accepted May 13, 1992

The study of the interactions between physical limitation by light and biological limitations in photobioreactors leads to very complex partial differential equations. Modeling of light transfer and kinetics and the assessment of radiant energy absorbed in photoreactors require an equation including two parameters for light absorption and scattering in the culture medium. In this article, a simple model based on the simplified, monodimensional equation of Schuster for radiative transfer is discussed. This approach provides a simple way to determine a working illuminated volume in which growth occurs, therefore allowing identification of kinetic parameters. These parameters might then be extended to the analysis of more complex geometries such as cylindrical reactors. Moreover, this model allows the behavior of batch or continuous cultures of cyanobacteria under light and mineral limitations to be predicted.
Key words: modeling • kinetics • cyanobacteria • photobioreactors • radiative transfer

INTRODUCTION

Mathematical modeling of photobioreactors requires the coupling between the metabolism of microorganisms and the physical phenomena of light transfer inside the culture medium to be known.

Photoreactors are governed by the availability of radiant light energy, which is very heterogeneous within the culture volume. This spatial heterogeneity results in local reaction rates and linear macroscopic kinetics, which makes it necessary to derive local equations and to calculate the total radiant energy absorbed by the cells. Generally, the Lambert law is assumed to express the attenuation of radiant energy flux resulting from light absorption by pigments in monodimensional applications.[4,5,8,14] However, this law, which neglects light scattering by particles, provides only first approximations for turbid cultures. Studies on solar energy conversion yield by photosynthetic microorganisms[3,6] have shown that a best accuracy could be obtained with the equation of radiative transfer. However, the complexity of this equation, even when applied to the simplified monodimensional geometry, requires long calculation times that hinder the identification of kinetic parameters.

Schuster[10] proposed a simplified, monodimensional equation of radiative transfer, incorporating two independent parameters related to light absorption and scattering. We used the analytical solution of this equation for the determination of local radiant energy available in the culture medium and for the approximate quantification of the total energy absorbed in the vessel. Schuster's approximations then enabled us to establish a simple mathematical model that accounts for light limitation during growth and for the transition of the kinetics of photosensitized reactions from exponential to linear.

Moreover, the resolution of the radiative transfer equation also simplifies studies of kinetic aspects related to other limitations that are of great interest, especially for mathematical modeling of closed ecological life support systems (CELSS). Mineral limitations, though controlling the process, are interrelated with light limitation since growth reactions occur only in the illuminated part of the bioreactor. The definition of kinetic parameters related to light or to mineral limitations therefore implies that this illuminated volume is known, particularly for batch cultures in which it changes during the time course of the experiment.

Accordingly, we also introduce in this article the concept of working illuminated volume, as defined from the expression of the transmittance given by the resolution of the radiative transfer equation. This concept allows

* To whom all correspondence should be addressed.

CCC 0006-3592/92/070817-09$04.00

the identification, in simple rectangular photobioreactors, of kinetic parameters, the use of which can be extended to studies of more complex geometries, such as cylindrical vessels.

MATERIALS AND METHODS

The cyanobacterium *Spirulina platensis* (strain 8005, Institut Pasteur) was axenically grown in a culture medium described by Zarrouk.[15] Biomass, including extracellular polysaccharide, was turbidimetrically determined at 750 nm using a dry weight conversion factor. Absorption and scattering mass coefficients were determined, according to Aiba[1] and Shibata,[11] with the opalescent plate method. Experimental results were computed using a Newton–Raphson algorithm to solve a nonlinear algebraic system.

All spectrophotometric determinations were performed with a UVIKON 860 spectrophotometer (KONTRON). Luminous fluxes were measured with a Li-185 B radiometer (Li-COR) through an infrared cutoff filter (350–750 nm).

LIGHT TRANSFER MODELS

Scope

Light energy dissipation inside a liquid medium taken to be nonemitting and nonfluorescing depends on two independent phenomena: absorption by the pigments and scattering by whole cells, often called the shading effect. This shading effect makes the mathematical description of light transfer extremely complex: The available energy at any point of the bioreactor comes from the main light source and from all space directions as light scattered by the suspension. Thus the absorbed energy depends on the scattering characteristics of the entire volume. The problem is accordingly described by an integro-differential system.[1-3,6,12,13]

Two approaches can be adopted: Either the use of an oversimplified model that neglects shading or the numerical integration of the integro differential problem by a Monte Carlo method that requires sophisticated numerical tools and long calculation times.[1,2] The present work attempts to develop an alternative way using a two-parameter model that remains mathematically tractable and that accounts independently for absorption and scattering.

Mathematical Background of the Light Transfer Problem in Monodimensional Geometries

The attenuation of light in batch or continuous cultures in photobioreactors creates a heterogeneous radiation field inside the culture responsible for local kinetics. It is therefore necessary to consider the effects on growth rate of the light intensity available at each point of the reactor. Monodimensional geometries simplify this problem by reducing the knowledge required to the projection of the vectors along one axis only, namely the z axis. Such an approximation is only possible for rectangular photoreactors in which light is provided on one side or two opposite sides. The specific light intensity of wavelength λ, $I_\lambda(z,\theta,\varphi)$, at each point of the z axis, in the direction making an angle θ with the z axis, with φ as the azimuthal angle in spherical coordinates (Fig. 1), characterizes the radiation field.

Assuming the radiation field is isotropic, the mean intensity $J_{z\lambda}$ is calculated by the double integral:

$$J_{z\lambda} = \frac{1}{4\pi} \iint I_\lambda(z,\theta)\, d^2\omega$$

where $d^2\omega$ denotes for the differential of the solid angle, $d^2\omega = \sin\theta\, d\theta\, d\varphi$ (Fig. 1), which leads to

$$J_{z\lambda} = \frac{1}{4\pi} \int_0^{2\pi} \int_0^{\pi} I_\lambda(z,\theta) \sin\theta\, d\theta\, d\varphi \qquad (1)$$

The radiant energy flux in the z direction is similarly calculated by

$$\mathbf{F}_{z\lambda} = \iint I_\lambda(z,\theta) \cos\theta\, d^2\omega$$

$$= \int_0^{2\pi} \int_0^{\pi} I_\lambda(z,\theta) \sin\theta \cos\theta\, d\theta\, d\varphi \qquad (2)$$

If the medium is assumed to be absorbing, scattering, nonemitting, and nonfluorescing, two parameters are necessary to characterize the path of the light. Also, the assumption that scattering and absorption are proportional to the biomass concentration introduces the absorption and scattering mass coefficients $E_{a\lambda}$ and $E_{s\lambda}$ (square meters per kilogram of biomass).

The light energy balance[2] upon a differential length dz (again assuming a monodimensional geometry) enables the variation of the radiant energy flux along the z axis

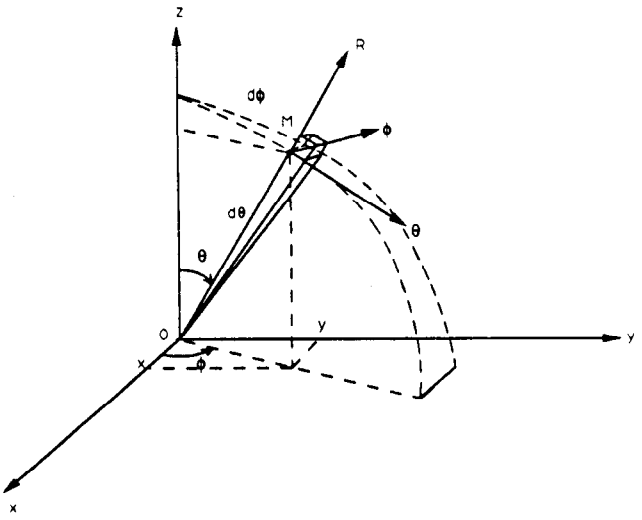

Figure 1. Profile of light radiant energy flux in monodimensional geometry.

to be related to the mean intensity:

$$\frac{d\mathbf{F}_{z\lambda}}{dz} = -4\pi E_{a\lambda} C_x J_{z\lambda} \tag{3}$$

The right-hand term represents the local absorption rate ($W \cdot m^{-4}$) noted, $A_{z\lambda}$, so that

$$A_{z\lambda} = 4\pi E_{a\lambda} C_x J_{z\lambda} \tag{4}$$

The above equations characterize the light energy dissipation in an isotropic radiation field for monodimensional geometry and for a radiation of wavelength λ; the definitions can be extended to the total emission spectrum by

$$I_z = \int_\lambda I_{z\lambda} d\lambda$$

and similarly for F_z, J_z, *and* A_z;

$$E_a = \frac{1}{\Delta\lambda} \int_\lambda E_{a\lambda} d\lambda$$

and similarly for E_s.

The Simplest Model: Beer–Lambert Equations

The Beer–Lambert law has usually been used to express the exponential attenuation of the radiant energy flux, which results from absorption by the culture medium only.[4,5,8,14] This model, extensively used in photometry, is based on two assumptions: (1) the light field remains parallel throughout the vessel and (2) the scattering of the solid particles can be neglected.

A differential radiant energy balance upon a cross-sectional area leads to

$$d\mathbf{F}_z = -E_{aL} C_x F_z dz$$

which after integration gives

$$\mathbf{F}_z = F_0 \exp(-E_{aL} C_x z) \tag{5}$$

The subscript L has been added to the absorption coefficient E_a to account for the fact that E_{aL} aggregates absorption and leaks of light energy by scattering; E_{aL} is generally termed the extinction coefficient.

Adaptation of Schuster's Hypotheses

The problem of radiative transfer which is expressed by the light energy balance [Eqs. (1)–(3)] is an integro-differential problem requiring sophisticated numerical methods for its solution. The computation method used has to be linked to time-dependent kinetic equations, leading to high complexity and requiring a long calculation time.

A simplified solution has been proposed by Schuster[10] which neglects the angular distribution of the incident intensity at the external walls and of the scattered intensity inside the medium. We can summarize his assumptions as (1) the light field remains isotropic throughout the vessel and (2) absorption and scattering are accounted for independently by the two coefficients E_a and E_s: The scattered intensity is assumed to be emitted by the suspended particles in the main direction of the radiation either positively or negatively.

The field of radiation is then split into two opposite fluxes F_z^+ and F_z^- assumed to be parallel to the z axis (Fig. 2). Two energy balances on the elemental volume of thickness Δz can be established separately for the direct and the reverse fluxes F_z^+ and F_z^-:

$$F^+|_z - F^-|_{z+\Delta z} + \tfrac{1}{2}E_s C_x \cdot \Delta z \cdot F^-|_z = E_a C_x \cdot \Delta z \cdot F^+|_z + \tfrac{1}{2}E_s C_x \cdot \Delta z \cdot F^+|_z \tag{6}$$

$$F^-|_{z+\Delta z} - F^-|_z + \tfrac{1}{2}E_s C_x \cdot \Delta z \cdot F^+|_z = E_a C_x \cdot \Delta z \cdot F^-|_z + \tfrac{1}{2}E_s C_x \cdot \Delta z \cdot F^-|_z \tag{7}$$

The coefficient 1/2 has been assigned to the scattering terms; in this form, the radiant energy balances state that half of the direct scattered energy $\frac{1}{2}E_s C_x \cdot \Delta z \cdot F^+|_z$ is reflected in the opposite direction F_z^- and must therefore be added as an entry term in the F_z^- balance. Conversely, the term $\frac{1}{2}E_s C_x \cdot \Delta z \cdot F^-|_z$ must be considered in the F_z^+ balance. By dividing the entire Eqs. (6) and (7) by Δz and taking the limit as Δz approaches zero, the following differential system is obtained:

$$\frac{dF_z^+}{dz} = -E_a C_x \cdot F_z^+ + \tfrac{1}{2}E_s C_x (F_z^- - F_z^+) \tag{8}$$

$$\frac{dF_z^-}{dz} = E_a C_x \cdot F_z^- + \tfrac{1}{2}E_s C_x (F_z^- - F_z^+) \tag{9}$$

This system of ordinary differential equations can easily be integrated, provided appropriate boundary conditions are expressed. If the reactor is illuminated on one side ($z = 0$) with parallel light and the opposite side ($z = L$) and the lateral sides are covered with an absorbing material such as black paper, the following boundary conditions can be set:

$$z = 0 \qquad F_z^+ = F_0 \tag{10}$$

$$z = L \qquad F_z^- = 0 \tag{11}$$

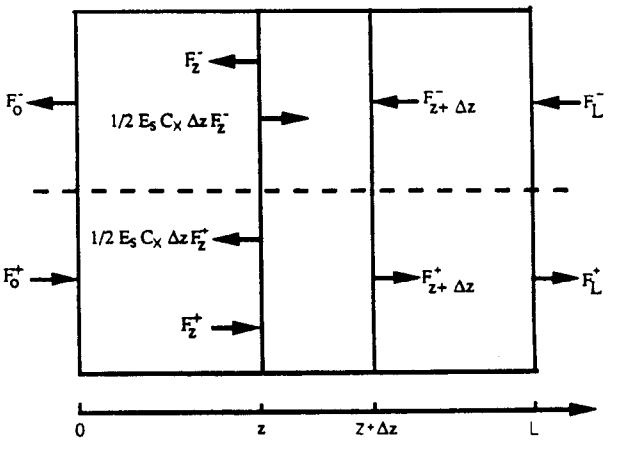

Figure 2. Global radiant energy balances on an elemental volume of thickness Δz.

The integration of Eqs. (8) and (9) with (10) and (11) is straightforward:

$$\frac{F_z^+}{F_0} = \frac{(1+\alpha)^2 \cdot e^{-\delta(Z-1)} - (1-\alpha)^2 \cdot e^{\delta(Z-1)}}{(1+\alpha)^2 \cdot e^{\delta} - (1-\alpha)^2 \cdot e^{-\delta}} \quad (12)$$

$$\frac{F_z^-}{F_0} = \frac{(1-\alpha^2)(e^{-\delta(Z-1)} - e^{\delta(Z-1)})}{(1+\alpha)^2 \cdot e^{\delta} - (1-\alpha)^2 \cdot e^{-\delta}} \quad (13)$$

where α and δ are given by

$$\alpha = [E_a/(E_a + E_s)]^{1/2} \quad (14)$$

$$\delta = (E_a + E_s)\alpha C_x L \quad (15)$$

and Z is the dimensionless abscissa z/L.

The radiant energy flux $\mathbf{F}_z$ is then obtained by the vectorial sum of the direct and reverse fluxes so that

$$\mathbf{F}_z = F_z^+ - F_z^- \quad (16)$$

The mean intensity J_z is calculated according to Eqs. (3), (8), (9), and (16), leading to the simple result that J_z is proportional to the absolute sum of F_z^+ and F_z^-:

$$J_z = \frac{1}{4\pi}(F_z^+ + F_z^-) \quad (17)$$

The choice of $\mathbf{F}_z$ or J_z to express the effects of light availability in the medium by a kinetic law is determinant, since it will modify the value of the light relative kinetic parameter. Physiologically, the value $4\pi J_z$ that represents the radiant energy available seems more appropriate. We thus chose to work with the quantity $F_z^+ + F_z^-$.

Using Eqs. (12) and (13), $4\pi J_z$ is then given by

$$\frac{4\pi J_z}{F_0} = 2\frac{(1+\alpha)e^{-\delta(Z-1)} - (1-\alpha)e^{\delta(Z-1)}}{(1+\alpha)^2 e^{\delta} - (1-\alpha)^2 e^{-\delta}} \quad (18)$$

The Z profiles of F_z^+/F_0, F_z^-/F_0, and $4\pi J_z/F_0$ have been plotted in Figures 3a–3c for $\delta/\alpha = (E_a + E_s)C_x \cdot L = 1$ and for three values of α. For $\alpha = 0$ (Fig. 3a, no absorption) the profiles are linear. This is the conservative case, and it is easily shown that $F^-|_{z=0} + F^+|_{z=L} = F_0$, which means that the radiant energy entering at $z = 0$ ($F^+|_{z=0} = F_0$) completely leaves the reactor in the positive direction, at $z = L$, and in the reverse direction, at $z = 0$. In addition, this figure confirms the balance of the conservative case that the energy flux $\mathbf{F}_z$ remains equal to F_0 throughout the medium. For $\alpha = 1$ (Fig. 3c, no scattering), the $F_z^{\pm}$ profile indicates an exponential decrease along the z axis that corresponds to the Beer–Lambert law [Eq. (5)].

The Z profile of the ratio $4\pi J_z/F_0$ is plotted in Figure 4 for $\alpha = 0.5$ and for several values of the parameter δ, which is proportional to the biomass concentration and to the thickness of the medium at fixed absorption and scattering conditions [Eq. (15)]. The results clearly indicate that as the biomass concentration increases, a large part of the photoreactor may become dark and thus inefficient. This fact will be used below to define a working volume inside the reactor.

Comparison between Schuster and Beer–Lambert Models

As previously mentioned, the expressions derived from Schuster's hypotheses contain the Beer–Lambert model assigning a value of 1 to the parameter α. The $\mathbf{F}_z$ and J_z profiles are obviously different for the two models; briefly speaking, Schuster's hypotheses enable gradual deviation from the exponential decay predicted by the Beer–Lambert law to the limit flat profile for $\mathbf{F}_z$ in the case of no absorption.

The two models can be compared more explicitly using measurable and/or average quantities such as the transmittance and the average volumetric rate at which energy is absorbed inside the medium.

The expression of the transmittance T is given by the ratio of the energy flux at $z = L$ over the incident flux F_0:

$$T = \frac{F_L}{F_0} = \frac{4\alpha}{(1+\alpha)^2 e^{\delta} - (1-\alpha)^2 e^{-\delta}} \quad (19)$$

Again setting $\alpha = 1$ for the Beer–Lambert model, it is always possible to identify one value of the extinction coefficient E_{aL} from a measured value of the transmittance at a fixed biomass concentration [accounted for by parameter δ via Eq. (15)]. Nevertheless, the variation of T with biomass concentration will not be correctly predicted by the Beer–Lambert model. Moreover, if the mass fraction of pigments in the biomass changes, for example because of mineral limitations, the values of α, and as a consequence the value of T, are strongly affected. Thus it may be concluded that Schuster's hypotheses afford an improvement of the robustness of the light transfer model for different biomass concentrations and different pigment compositions of biomass.

The average volumetric rate $\langle A \rangle$ at which energy is absorbed inside the bioreactor can be expressed in three ways. Considering the macroscopic energy balance of light over the entire reactor,

$$\frac{\langle A \rangle}{(F_0/L)} = 1 - \frac{F_L^+}{F_0} - \frac{F_0^-}{F_0} \quad (20)$$

which leads to [Eqs. (12) and (13)]:

$$\frac{\langle A \rangle}{(F_0/L)} = 1 - \left[\frac{4\alpha + (1-\alpha^2)(e^{\delta} - e^{-\delta})}{(1+\alpha)^2 e^{\delta} - (1-\alpha)^2 e^{-\delta}}\right] \quad (21)$$

The average volumetric rate at which energy is absorbed can also be expressed by

$$\langle A \rangle = \frac{1}{L}\int_0^L A_z\, dz$$

Using Eqs. (4), (14), and (15),

$$\frac{\langle A \rangle}{(F_0/L)} = \frac{\alpha\delta}{F_0}\int_0^1 4\pi J_z\, dZ$$

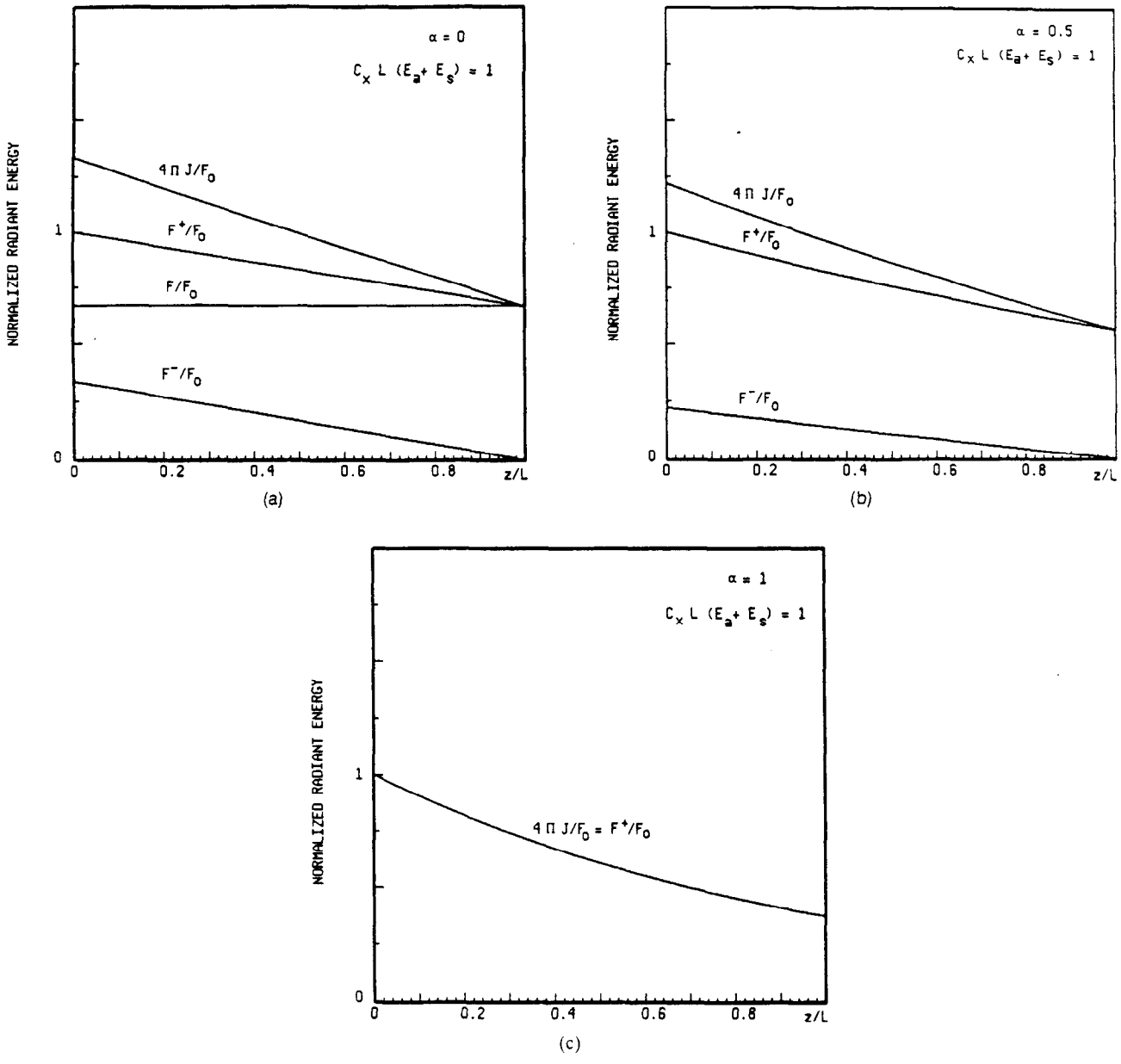

Figure 3. Profiles in normalized radiant energy available, $4\pi J_z/F_0$: (a) scattering medium ($\alpha = 0$); (b) absorbing and scattering medium ($\alpha = 0.5$); (c) absorbing medium ($\alpha = 1$); $Z = z/L$ is the dimensionless thickness of the medium.

which enables the average available energy $\langle 4\pi J \rangle$ to be simply calculated:

$$\langle 4\pi J \rangle = \frac{1}{L}\int_0^L 4\pi J_z\, dz = \frac{F_0}{\alpha\delta}\left[1 - \frac{4\alpha + (1-\alpha^2)(e^{\delta} - e^{-\delta})}{(1+\alpha)^2 e^{\delta} - (1+\alpha)^2 e^{-\delta}}\right] \quad (22)$$

The third way uses Eqs. (3) and (4):

$$\frac{\langle A \rangle}{(F_0/L)} = -\int_{F_0}^{F_L} \frac{d\mathbf{F}_z}{F_0}$$

which gives the same result as Eq. (21). The ratio $\langle A \rangle/(F_0/L)$, i.e., the reduced absorbed energy rate, is plotted in Figure 5 for different values of parameter α versus the ratio δ/α, which represents a dimensionless amount of biomass inside the reactor. The ratio $\langle A \rangle/(F_0/L)$ asymptotically reaches a maximum value as the biomass quantity increases, which confirms that the reactor performance may be limited by light energy transfer when biomass concentrates in the medium. It is easily established that the asymptotic value of $\langle A \rangle/(F_0/L)$ is given by

$$\lim_{C_x, L \to \infty}\left[\frac{\langle A \rangle}{(F_0/L)}\right] = \frac{2\alpha}{1+\alpha} \quad (23)$$

Similarly, the asymptotic value of the average intensity becomes

$$\lim_{C_x, L \to \infty} \langle 4\pi J \rangle = F_0 \frac{2}{1+\alpha} \quad (24)$$

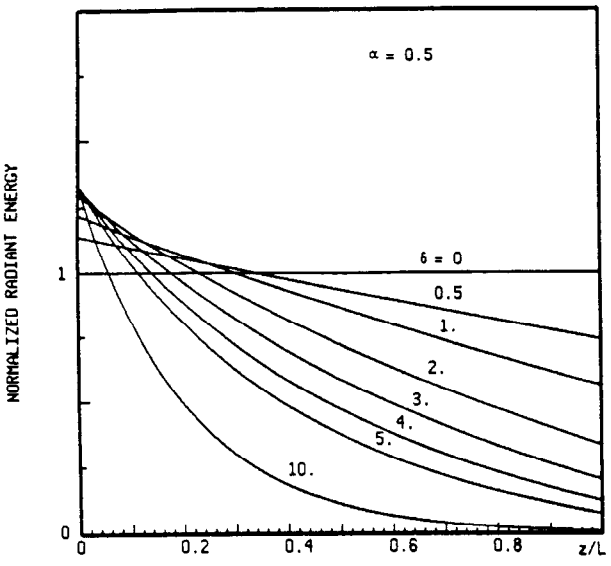

Figure 4. Profiles in normalized radiant energy available, $4\pi J_z/F_0$, versus the dimensionless thickness of the medium, z/L: $\alpha = 0.5$; δ as parameter.

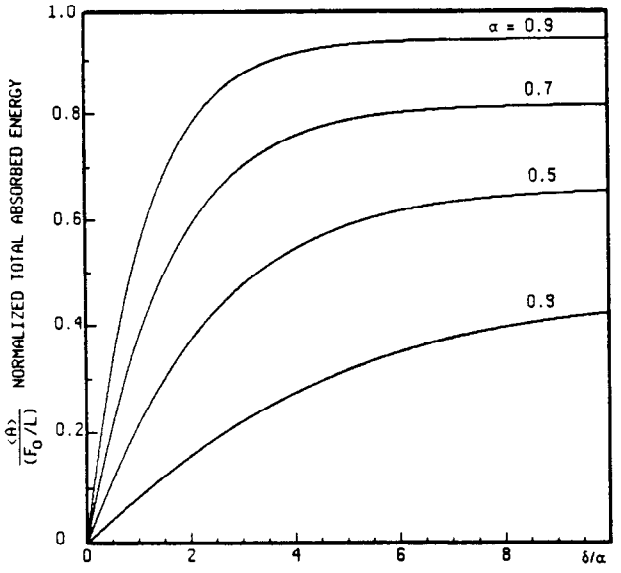

Figure 5. Normalized absorbed energy rate into the photobioreactor versus the ratio δ/α (normal optical thickness); α as a parameter.

For small biomass concentrations ($\delta \to 0$), Taylor expansions in Eqs. (21) and (23) lead to

$$\lim_{C_x \to 0} \left[\frac{\langle A \rangle}{(F_0/L)} \right] = \alpha\delta = E_a \cdot C_x \cdot L \tag{25}$$

$$\lim_{C_x \to 0} \langle 4\pi J \rangle = F_0 \tag{26}$$

It is obvious from Figure 5 and from Eqs. (23) to (25) that the Beer–Lambert and the present models furnish different results. As regards the light energy uptake by the microorganisms in the photobioreactor, it is necessary to characterize absorption and scattering separately. As a consequence, the Beer–Lambert model would lead to erroneous calculation of light energy conversion yields.

Therefore, Schuster's approximations afford analytical expressions accounting independently for absorption and scattering and improve considerably on the simpler model of Beer–Lambert.

COUPLING GROWTH KINETICS AND LIGHT TRANSFER MODELS

The absorption of light by pigments in high concentration may create a dark zone in photobioreactors in which growth will not occur. The existence of a radiant energy profile in the illuminated zone results in a mean growth rate that can be calculated with a mean volumetric integral, assuming a kinetic law for growth. Growth rate versus the radiant energy flux $\mathbf{F}_z$ is generally taken to follow a Monod-type law.[5,8,9,14] As mentioned above, we prefer to work with the total available energy $4\pi J_z$:

$$r_x = \mu_M \cdot C_x \frac{4\pi J_z}{K_J + 4\pi J_z} = \mu \cdot C_x \tag{27}$$

The mean biomass volumetric rate is then given by

$$\langle r_x \rangle = \frac{1}{V} \iiint_V r_x \cdot dV \tag{28}$$

$$\langle r_x \rangle = \frac{1}{V} \iiint_V \mu_M \cdot C_x \frac{4\pi J_z}{K_J + 4\pi J_z} \cdot dV \tag{29}$$

and in monodimensional photobioreactors

$$\langle r_x \rangle = \frac{1}{L} \int_0^L \mu_M \cdot C_x \cdot \frac{4\pi J_z}{K_J + 4\pi J_z} \cdot dz \tag{30}$$

It must be emphasized that light energy limitation is the most commonly encountered condition during culture of photosynthetic bacteria or algae, even when light energy is available in the entire reactor volume.

For low-energy inputs, the incident energy F_0 is negligible compared to K_J, which means that the specific growth rate μ is proportional to $4\pi J$ throughout the illuminated volume. In monodimensional applications, Eq. (27) therefore becomes

$$r_x = \frac{4\pi \cdot \mu_M}{K_J} \cdot C_x \cdot J_z \tag{31}$$

The mean volumetric growth rate then can be calculated assuming Schuster's approximations adequately characterize light scattering in the medium. Two limiting cases can be examined:

If the biomass concentration is low, then using Eq. (26), we obtain

$$\langle r_x \rangle = \frac{\mu_M}{K_J} \cdot F_0 \cdot C_x \tag{32}$$

Although the metabolism is limited by light energy, growth is exponential, with an apparent maximum specific growth rate $\mu_M \cdot F_0/K_J$ proportional to the incident energy and independent of the absorption and scattering characteristics of the medium.

If the biomass concentration is high; using Eq. (24), we obtain

$$\langle r_x \rangle = \frac{\mu_M}{K_J} \cdot \frac{F_0}{E_a \cdot L} \cdot \frac{2\alpha}{1 + \alpha} \tag{33}$$

The growth rate is independent of the biomass concentration, indicating a linear growth, the rate of which is strongly dependent on the absorption and scattering characteristics of the medium (E_a and α) and proportional to the incident energy F_0.

When the approximation $K_J \gg F_0$ can no longer be made, the mean growth rate [Eq. (30)] must be numerically calculated using the appropriate equation for $4\pi J_z$ [Eq. (18)]. The ratio $\langle r_x \rangle / \mu_M$ is reported in Figure 6 versus the biomass concentration with F_0/K_J as a parameter. The exponential growth ($\langle r_x \rangle / \mu_M$ proportional to C_x) and the linear growth ($\langle r_x \rangle / \mu_M$ independent of C_x) are conserved, whatever the ratio F_0/K_J, but the limit expressions for linear growth rate [Eq. (32)] and specific maximum growth rate [Eq. (33)] do not remain valid.

The value of the ratio μ_M/K_J can easily be determined from a batch growth experiment for limiting values of radiant energy from measurements of either exponential [Eq. (32)] or linear [Eq. (33)] growth. It must be emphasized that the identification cannot be performed without stating a light energy absorption and scattering model, requiring simple geometries such as monodimensional reactors. It is noteworthy that the Beer–Lambert and Schuster models will lead to the same results, as regards growth, if the extinction coefficient E_{aL} is equal to [Eq. (33)]

$$E_{aL} = E_a \frac{1 + \alpha}{2\alpha} \tag{34}$$

The results given by this equation differ from those obtained from physical measurements of the transmittance [Eq. (19)], which again confirms the improvement of the light transfer model developed using Schuster's assumptions.

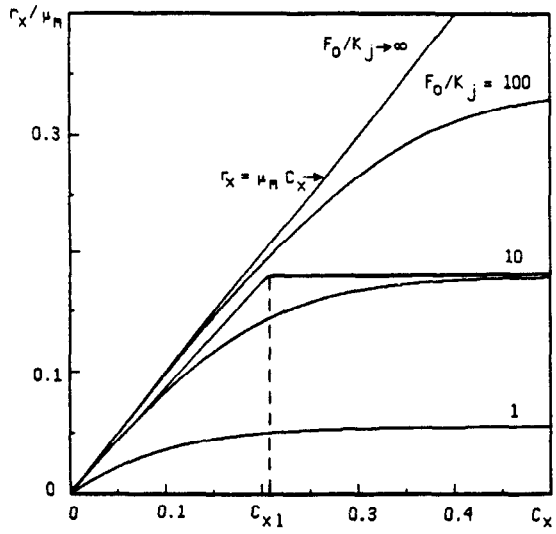

Figure 6. Dimensionless growth rate r_x/μ_M (kg · m^{-3}) versus biomass concentration C_x (kg · m^{-3}): $E_a = E_s = 200$ m^2 · kg^{-1}; $L = 0.05$ m; F_0/K_J as a parameter. Graphical determination of C_{x1}.

WORKING ILLUMINATED VOLUME

The preceding developments can be further simplified by introducing the concept of a working illuminated volume, which divides the photobioreactor into a dead zone in which no metabolic activity is supposed and an illuminated zone in which growth occurs.

We define the working illuminated volume as the volume in which growth would be exponential, the other part of the bioreactor being inactive. The average volumetric rate is expressed by

$$r_x = (1 - \gamma)\frac{1}{V_1}\iiint_{v1} r_{x1}\,dV + \gamma\frac{1}{V_2}\iiint_{v2} r_{x2}\,dV \tag{35}$$

where subscripts 1 and 2 refer to the dark and the illuminated zones, respectively; γ stands for the ratio of illuminated volume to total volume. Given that respiration of cyanobacteria is inhibited in the light[7] and assuming that the residence time of cells in darkness is short enough to avoid respiration, $r_{x1} = 0$. In monodimensional applications, $\gamma = L_2/L$, Eq. (35) becomes

$$\langle r_x \rangle = \gamma \cdot \frac{1}{L_2}\int_0^{L_2} r_{x2} \cdot dz \tag{36}$$

Two cases have to be examined: $F_0 \ll K_J$ and the general case.

For low-energy inputs, the approximation $F_0 \ll K_J$ already discussed is valid. The volumetric growth rate in the working illuminated volume r_{x2} is then given by Eq. (32); $\langle r_x \rangle$ is then expressed by

$$\langle r_x \rangle = \frac{L_2}{L}\frac{\mu_M}{K_J}F_0 C_x \tag{37}$$

If a dark zone does exist, the overall growth is linear and the average growth rate is also expressed by Eq. (33). Combining the two expressions for $\langle r_x \rangle$ affords the working illuminated length L_2 as

$$L_2 = \frac{2\alpha}{1 + \alpha}\frac{1}{E_a C_x} \tag{38}$$

The most important fact is that the working length L_2 is independent of incident energy F_0, kinetic parameters μ_M and K_J, and the reactor thickness L. Thus L_2 is a lumped parameter that takes into account the relative influence of absorption and scattering and the biomass concentration.

In the general case, it is always possible to define exponential linear growth phases, as mentioned above, even though no analytical expression for $\langle r_x \rangle$ can be derived. Nevertheless, a limiting value of parameter δ can be calculated graphically by the intercept of the line $\langle r_x \rangle = k_1 \mu_M \delta$ and the line $\langle r_x \rangle = k_2$ (Fig. 6). The obtained value δ_M corresponds to the maximum value of δ

and therefore to the limit value of the biomass concentration C_{x1} that could be obtained by exponential growth in a hypothetical bioreactor uniformly lit throughout its entire volume with energy flux F_0. When the linear growth is observed, the biomass concentration C_x is larger than C_{x1} so that the behavior of the culture is equivalent to that of a hypothetical bioreactor of thickness L_2 smaller than total thickness L where biomass at a concentration C_x would grow exponentially consuming the same light energy. The light energy consumption is given by the product $\langle A \rangle V$, which in turn means that for monodimensional applications the product $\langle A \rangle L$ reaches a constant value. At fixed α and F_0, this means that δ remains equal to δ_M if the biomass concentration is greater than C_{x1} [Eq. (21)]. As a consequence, the transmittance T [Eq. (19)] and the average available energy $\langle 4\pi J_z \rangle$ [Eq. (23)] remain unchanged. The working illuminated thickness L_2 is then given by [Eq. (15)]:

$$L_2 = \frac{C_{x1}}{C_x} L \tag{39}$$

Equation (38) corresponds to the limit expression of Eq. (39) when $F_0 \ll K_J$.

Different values of C_{x1} were graphically determined from batch cultures of *S. platensis* for two different rectangular bioreactors (Roux flasks of thicknesses 0.05 and 0.08 m) and radiant energy fluxes F_0 that varied between 4 and 20 W · m^{-2}. It is interesting to note that the values obtained correspond to a constant value of energy flux at $z = L$, F_L, calculated from the transmittance ratio [Eq. (19)]. The value of F_L obtained from eight independent experiments is

$$F_L = 4\pi J_L = 1.0 \pm 0.1 \text{ W} \cdot \text{m}^{-2}$$

The concept of a working illuminated length L_2 can easily be extrapolated to multidimensional reactors, i.e., to a working volume, assuming L_2 represents an operative thickness. Although hypotheses of the Schuster model [Fig. 2 and Eqs. (8) and (9)] are no longer satisfied, this kind of approximation may provide a useful framework for situations of complex light transfer. For a cylindrical reactor of external diameter D, with a radial illumination, the parameter γ is given by

$$\gamma = \frac{4L_2(D - L_2)}{D^2} \tag{40}$$

CONCLUSION

The simplified model for radiative transfer developed in Eqs. (8)–(11) enables the radiant energy flux and the radiant energy available inside a monodimensional photoreactor to be calculated using a tractable system of algebraic equations. Schuster's approximations thus appear to be the simplest way to approach the radiant energy profile in the culture while taking into account the effect of biomass concentration and of the two independent absorption and scattering phenomena. This approach provides a useful framework for studying the effect of light intensity on the growth and metabolic behavior of photosynthetic microorganisms. However, it must be pointed out that the applicability of the model is limited to monodimensional applications and to a mean wavelength of the visible spectrum.

More sophisticated mathematical and numerical tools are required to solve, for each relevant wavelength, the exact equation of radiative transfer in its tridimensional form. However, this approach to precise calculation of the energy absorbed by the cells[1] requires very high calculation time and complex algorithms. Monodimensional operating conditions and the model developed in this article therefore appear to be the best approach for the identification of kinetic parameters.

This work was supported by the Centre National d'Etudes Spatiales and by the European Space Agency.

NOMENCLATURE

A	local absorption rate (W · m^{-3})
A_λ	local absorption rate for the radiation of wavelength λ (W · m^{-4})
C_x	biomass concentration (kg · m^{-3})
D	diameter (m)
E_a	global absorption mass coefficient (m^2 · kg^{-1})
E_s	global scattering mass coefficient (m^2 · kg^{-1})
E_{aL}	extinction coefficient of Beer–Lambert (m^2 · kg^{-1})
F	radiant energy flux (W · m^{-2})
F_λ	radiant energy flux for the radiation of wavelength λ (W · m^{-3})
I	specific intensity (W · m^{-2})
I_λ	specific intensity for the radiation of wavelength λ (W · m^{-3})
J	mean intensity (W · m^{-2})
J_λ	mean intensity for the radiation of wavelength λ (W · m^{-3})
K_J	half saturation constant for total energy available (W · m^{-2})
L	length of reactor (m)
L_2	length of working illuminated volume (m)
r_x	volumetric rate in biomass (kg · m^{-3} · h^{-1})
T	transmittance (dimensionless)
t	time (h)
V	volume (m^3)
z	length (m)
Z	dimensionless length, $=z/L$ (dimensionless)
$\langle\rangle$	mean volumetric integral, $= 1/V \iiint_V \cdot dV$

Greek letters

α	$(E_a/(E_a + E_s))^{1/2}$ (dimensionless)
γ	illuminated fraction of bioreactor volume (dimensionless)
δ	$(E_a \cdot (E_a + E_s))^{1/2} C_x L$ (dimensionless)
λ	wavelength (m)
μ	growth rate (h^{-1})
μ_M	maximum growth rate (h^{-1})
θ, φ	angle (rad)

References

1. Aiba, S. 1982. Growth kinetics of photosynthetic microorganisms. Adv. Biochem. Eng. **23**: 85–156.
2. Chandrasekhar, S. 1960. Radiative transfer. Dover Publications, New York.

3. Daniel, K. J., Laurendeau, N. M., Incropera, F. P. 1979. Predictions of radiation absorption and scattering in turbid water bodies. ASME J. Heat Transfer **101**: 63–67.
4. Fredrikson, A. G., Brown, A. H., Miller, R. L., Tsuchiya, H. M. 1961. Optimum conditions for photosynthesis in optically dense cultures of algae. ARS J. 1429–1435.
5. Frohlich, B.T., Webster, J. A., Attai, M. M., Shuler, M. L. 1983. Photobioreactors: Models for interaction of light intensity, reactor design and algal physiology. Biotechnol. Bioeng. Symp. **13**: 331–350.
6. Incropera, F. P., Thomas, J. F. 1978. A model for solar radiation conversion to algal in a shallow pond. Solar Energy **20**: 157–165.
7. Jones, L.W., Myers, J. 1963. A common link between photosynthesis and respiration in a blue-green alga. Nature **199**: 670–672.
8. Ogawa, T., Kozasa, H., Terui, G. 1971. Studies on the growth of *Spirulina platensis* (II). J. Ferment. Technol. **50**: 143–149.
9. Ogawa, T., Terui, G. 1970. Studies on the growth of *Spirulina platensis* (I). J. Ferment. Technol. **48**: 361–367.
10. Schuster, A. 1905. Radiation through a foggy atmosphere. Astrophys. J. **21**: 1–22.
11. Shibata, K. 1958. Spectrophotometry of intact biological material. J. Biochem. **45**: 599–623.
12. Siegel, R., Howell, J. R. 1981. Thermal radiation heat transfer. 2nd edition. Hemisphere publishing, McGraw-Hill, New York.
13. Spadoni, G., Bandini, E., Santarelli, F. 1978. Scattering effects in photosensitized reactions. Chem. Eng. Sci. **33**: 517–524.
14. Ten Hoopen, H. G. J., Roels, J. A., Van Gemert, J. M., Nobel, P. J., Fuchs, A. 1981. An unstructured model of algal growth in continuous cultures. pp. 315–321 In: Advances in biotechnology. International Fermentation Symposium. Pergamon, Elmsford, N Y.
15. Zarrouk, C. 1966. Contribution à l'étude d'une cyanophycée. Influence de divers facteurs physiques et chimiques sur la croissance et la photosynthèse de *Spirulina maxima* (Setch et Gardner) *Geitler*. Ph.D. Thesis, Université de Paris.

A Structured Model for Simulation of Cultures of the Cyanobacterium *Spirulina platensis* in Photobioreactors: II. Identification of Kinetic Parameters under Light and Mineral Limitations

J. F. Cornet
Matra-Espace—Applications de la microgravité, 78146 Vélizy-Villacoublay, France

C. G. Dussap*
Laboratoire de Génie Chimique Biologique, Université Blaise Pascal, Clermont II, 63177 Aubière Cédex, France

P. Cluzel and G. Dubertret
Laboratoire de Biochimie Fonctionnelle des Membranes Végétales, C.N.R.S., 91198 Gif-sur-Yvette Cédex, France

Received August 29, 1991/Accepted May 13, 1992

A structured model for the culture of cyanobacteria in photobioreactors is developed on the basis of Schuster's approximations for radiative light transfer. This model is therefore limited to monodimensional geometries and kinetic aspects.

Light-harvesting pigments play a crucial role in defining the profile of radiative transfer inside the culture medium and in controlling the metabolism, particularly the metabolic deviations induced by mineral limitations. Modeling therefore requires the biomass to be divided into several compartments, among which the light-harvesting compartment allows a working illuminated volume to be defined within the photobioreactor. This volume may change during batch cultures, largely decreasing as pigment concentration increases during growth but increasing as pigments are consumed during mineral limitation. This approach enables, in photobioreactors of simple parallelepipedic geometries, kinetic parameters to be determined with high accuracy; this may then be extended to vessels of more complex geometries, such as cylindrical photobioreactors.

The model is applied to controlled batch cultures of the cyanobacterium *Spirulina platensis* in parallelepipedic photobioreactors to assess its ability to predict the behavior of these microorganisms in conditions of light and mineral limitations. Results allowed the study of optimal operating conditions for continuous cultures to be approached. © 1992 John Wiley & Sons, Inc.

Key words: Modeling • kinetics • cyanobacteria • photobioreactors • *Spirulina platensis* • mineral limitations

INTRODUCTION

Mineral limitations during batch cultures of cyanobacteria result in marked metabolic deviations, which considerably modify the accumulation time courses of main biomass components (e.g., proteins, pigments,[2,3,14] carbohydrates[9]).

Phycocyanins are chromoproteins that constitute the main light-harvesting pigment in cyanobacteria and which represent about a quarter of the cell proteins. They are of special interest for modeling photobioreactors, since they play a crucial role in photosensitized photosynthetic reactions and are consumed under mineral starvation (N or S). As mentioned in the preceding report,[7] the proportion of light-absorbing pigments in the biomass allows a working illuminated volume to be defined within the photobioreactor in which photosensitized reactions take place.

However, the whole biomass participates in defining light characteristics within the photobioreactor by scattering light out of the vessel in proportions that have to be known for the assessment of total radiant energy absorbed in the reactor.

These typical interactions between the metabolism of microorganisms and physical phenomena require independent classes of biomass components to be defined for modeling. In such structured models,[12] biomass is divided into major components and kinetic laws are postulated. In the case of microalgae cultures in photobioreactors, under light and mineral limitations, introduction of a working illuminated volume in this type of model allows the different mean volumetric rates to be calculated, as explained in the preceding article.[7] This step therefore requires physical considerations on radiative transfer.

With a view to link the mean volumetric rates of substrate consumption to biomass synthesis, the mass conversion yields are theoretically established by writing stoichiometric equations for the formation of biomass and products from CO_2 and minerals.

* To whom all correspondence should be addressed

Biotechnology and Bioengineering, Vol. 40, Pp. 826–834 (1992)

CCC 0006-3592/92/070826-09$04.00

MATERIALS AND METHODS

The cyanobacterium *Spirulina platensis* strain 8005 (Institut Pasteur) was axenically grown in a culture medium described by Zarrouk,[15] but containing 10.5 kg · m^{-3} $NaHCO_3$ and 7.6 kg · m^{-3} Na_2CO_3. For studies of mineral limitations, nitrate concentration was reduced to 0.29 kg · m^{-3}, and sulfate was only provided by the inoculum.

Batch cultures were carried out in a 4-L parallelepipedic photobioreactor. Light was provided from one side by four white fluorescent lamps (Mazdafluor, industry white TF, 20 W). The opposite side was covered with black paper to comply with the light transfer model.[7]

Standard culture conditions were pH 9.5 ±0.1, temperature 36 ±1°C, air flow rate 1.6×10^{-5} $Nm^3 \cdot s^{-1}$. For cultures under sulfur limitation, the light flux was 18 W · m^{-2}; for nitrogen limitation, it was set at 8 and 12 W · m^{-2} in order to evaluate the effect of both nitrogen and light energy limitations.

Biomass, including extracellular polysaccharide, was turbidimetrically determined at 750 nm using a conversion factor for dry weight. Total proteins and total sugars were spectrophotometrically quantified with the BCA test (Pierce) and with the anthrone reagent,[8] respectively. Chlorophyll *a* and phycocyanin concentrations were calculated from a comparison of absorbances at 620 and 678 nm and corrected for scattering.[5,10] Nitrate and sulfate concentrations were determined according to the spectrophotometric method at 210 nm[6] and the sodium rhodizonate method,[13] respectively.

All spectrophotometric determinations were performed with a UVIKON 860 spectrophotometer (KONTRON). Light fluxes were measured with a LI-185 B radiometer (LI-COR) through an infrared cutoff filter (350–750 nm).

RESULTS

Eight experiments were performed in Roux flasks 0.05 and 0.08 m thick for incident light fluxes F_0 ranging between 4 and 20 W · m^{-2}; nitrogen and sulfur limitations were examined. Table I summarizes the different experimental conditions that were tested. For each experiment a linear growth phase was attained,[7] the rate of which is calculated in Table I, indicating a strong influence of F_0. Experiments 4 and 5 were performed in the same light conditions and are fairly reproducible. Nitrogen limitation was obtained for experiments 1 and 3; sulfur limitation was obtained for experiment 2.

Points on Figures 1 and 2 correspond to experimental measurements during growth of *Spirulina* under N and S depletion. For each culture, the percentage of N or S recovery was respectively 96% and 91%, confirming that all main molecular species involved initially in the process were correctly identified.

The measured effects of nitrate and sulfate limitations on batch cultures in a parallelepipedic photobioreactor were quite similar and in good agreement with those for nonfixing nitrogen cyanobacteria.[2-4] In the presence of nitrate and sulfate, both growth and accumulation of main cellular components were initially exponential and rapidly became linear as a result of light limitation by increasing self-shadowing. As soon as nitrate and sulfate were exhausted, phycocyanins (PC) (the main light-harvesting chromoprotein) began to be degraded, at a rate that was shown to be similar to that of their synthesis during the linear phase. This strongly suggests that the rate of PC degradation during limitation and the rate of PC synthesis during the linear growth phase are both related to the working illuminated volume.

However, N and S limitations exert different effects on the evolution of the overall protein composition. Under N starvation, the total amount of proteins in the culture stabilized to steady-state level, indicating that, as expected, PCs are used as N reserve for the continued synthesis of other proteins. On the other hand, the decrease in the total protein level observed during S starvation results from the degradation of both PCs and other proteins.

In both cases, a marked residual biomass accumulation originated in a very large synthesis of carbohydrates, probably as intracellular sulfated glycogen.

These data were used to establish the main hypothesis of the kinetic modeling.

MODELING: STRUCTURED MODELS OF KINETICS UNDER MINERAL LIMITATIONS

Structured Models

Structured models, including compartments, have been developed by Roels.[12] They are of particular interest in

Table I. Experimental conditions for the culture of *Spirulina platensis* in Roux flasks.

Experiment no.	Limitation	$L \times 100$ (m)	F_0 (W · m^{-2})	$r_x \times 10^3$ (kg · m^{-3} · h^{-1})	Experiments taken for identification					
					K_I	μ'_M	K_N	K_S	K_{PC}	q
1	N	8	20	3.2	+	+	+		+	
2	S	8	18	2.5	+	+		+	+	+
3	N	8	12	2.1	+	+	+		+	
4	—	8	11	1.8	+	+				
5	—	8	11	1.8	+	+				
6	N	8	8	1.7	+	+	+		+	
7	—	5	7	1.6	+	+				
8	—	5	4	1.5	+	+				

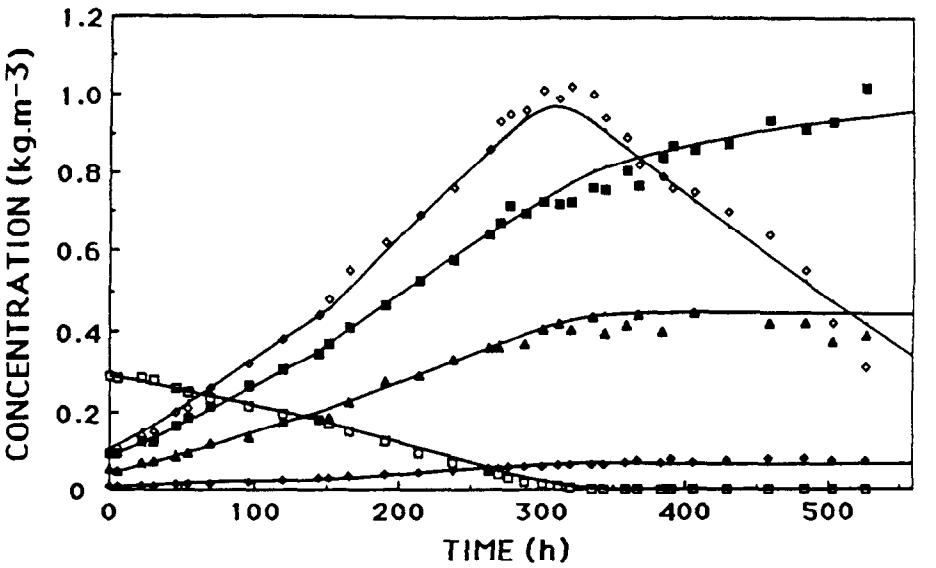

Figure 1. Batch culture of *S. platensis* in photobioreactor under NO_3^- depletion. Comparison between experimental data and the simulation obtained by the mathematical model (Table III): (■) Biomass concentration (kg · m^{-3}), (□) nitrate concentration (kg · m^{-3}), (▲) protein concentration (kg · m^{-3}), (◇) phycocyanin concentration (kg · m^{-3}, ×10), (◆) chlorophyll *a* concentration (kg · m^{-3}, ×10); F_0 is 8 W · m^{-2} before 144 h and 12 W · m^{-2} after.

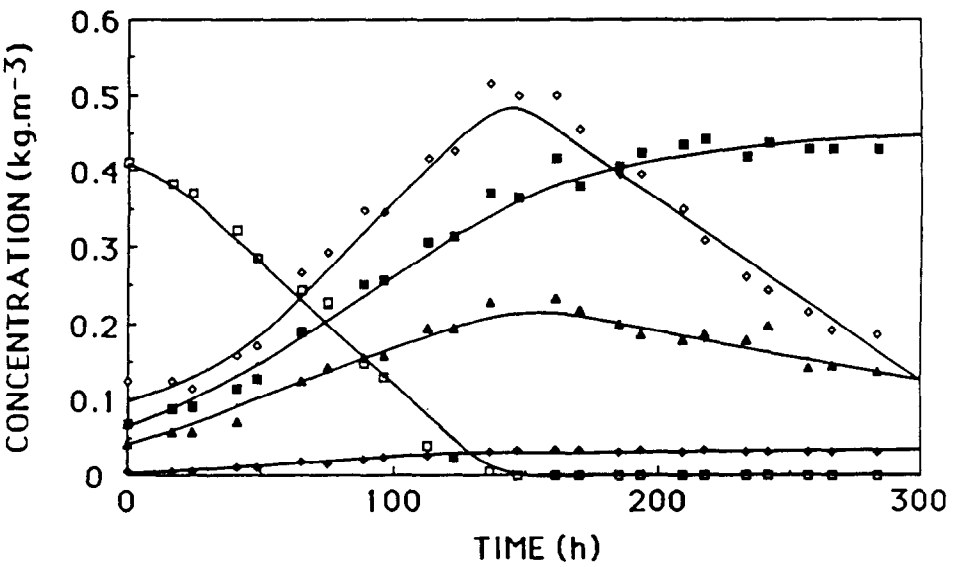

Figure 2. Batch culture of *S. platensis* in photobioreactor under SO_4^{2-} depletion. Comparison between experimental data and the simulation obtained by the mathematical model presented. (■) biomass concentration (kg · m^{-3}), (□) sulfate concentration (kg · m^{-3}, ×50), (▲) protein concentration (kg · m^{-3}), (◇) phycocyanin concentration (kg · m^{-3}, ×10), (◆) chlorophyll *a* concentration (kg · m^{-3}, ×10); F_0 = 18 W · m^{-2}.

our case, since some biomass components, such as pigments, play a crucial role in the behavior of the culture. If the concentration of biomass in the culture is C_x, the state of the culture is described by an overall chemical state vector **C**, which includes the concentrations of the compounds present in the biotic and abiotic phases. This state vector can be subdivided into a biotic state vector **X** and an abiotic vector **Y**. The different compounds of the biotic and abiotic phases that have been chosen for inclusion in our model are shown in Table II. The active biomass XA stands for the biomass as long as no limitation occurs, and the total biomass XT includes the additional intracellular glycogen appearing during mineral limitation (Table II).

For convenience and because it is easier to work with experimentally measured variables, the biotic state vector will be

$$\mathbf{X} = (C_{PC}, C_P, C_{CH}, C_{XA}, C_G)$$

and the abiotic state vector will be

$$\mathbf{Y} = (C_N, C_S)$$

Table II. Structured model.

Biotic phase

Active biomass XA				Sulfated intracellular glycogen G
Total proteins P		Chlorophylls		
Phycocyanins PC (PSII)	Other proteins OP	CH (PSI)	Biomass B	
Total biomass XT				

Abiotic phase

Nitrates N	Sulfates S

The state vector therefore is

$$\mathbf{C} = (C_{PC}, C_P, C_{CH}, C_{XA}, C_G, C_N, C_S)$$

where C expresses a concentration in kilograms per cubic meter. In addition, we can define the mass biotic fraction of compound i as $z_i = C_i/C_{XA}$ and the total biomass $C_{XT} = C_{XA} + C_G$.

Before the appearance of the limitation by sulfur or nitrogen, experimental results indicate that the biotic mass fractions of proteins (z_P), of phycocyanins (z_{PC}), and of chlorophylls (z_{CH}) remain constant whatever the energy flux, either in exponential or in linear growth phases (Figs. 1 and 2):

$$z_P = 0.57 \text{ kg P/kg } XA$$

$$z_{PC} = 0.135 \text{ kg PC/kg } XA$$

$$z_{CH} = 0.0085 \text{ kg CH/kg } XA$$

Some assumptions can be made here:

1. The C, H, O, N, S, and P elemental composition of the active biomass XA remains constant; this assumption has been experimentally confirmed for exponential and linear growth phases; under limiting conditions, i.e., for stationary phases, this assumption is assumed to remain valid.
2. The biotic mass fraction of proteins remains constant under N starvation but decreases under S starvation.
3. The biotic mass fraction of chlorophylls remains constant under N or S starvation.
4. The biotic mass fraction of phycocyanins decreases under N or S starvation.

Thus, z_P, z_{PC}, and z_{CH} may vary under N or S starvation, leading to change in the intrinsic compositions of biomass without any effect on the overall elemental composition.

Stoichiometry

Measurements of the elemental composition of *Spirulina* afforded the following C-molar formula for the active biomass:

$$CH_{1.650}O_{0.531}N_{0.170}S_{0.007}P_{0.006}$$

This formula, which includes extracellular polysaccharide, gave the following stoichiometric equation for photosynthesis:

$$CO_2 + 0.724H_2O + 0.170HNO_3 + 0.007H_2SO_4 + 0.006H_3PO_4 \longrightarrow CH_{1.650}O_{0.531}N_{0.170}S_{0.007}P_{0.006} + 1.378O_2$$

1. This equation is a pure equation for photosynthesis, since it has been shown that, as in all phototrophic prokaryotes,[11] respiration of *S. platensis* is inhibited by light.
2. Unlike the case of respiration, the elemental mass balance of this equation does not require experimentally determined conversion yields; this stoichiometric relation has therefore been established with zero degree of freedom and is entirely predictive, since the six stoichiometric coefficients were calculated from the six conservation balances of the C, H, O, N, S, and P balances.

Taking into account pH modifications during growth and using an oxidoreduction balance, this equation can be rewritten as

$$HCO_3^- + 0.724H_2O + 0.170NO_3^- + 0.007SO_4^{2-} + 0.006HPO_4^{2-} + 0.196H^+ \longrightarrow CH_{1.650}O_{0.531}N_{0.170}S_{0.007}P_{0.006} + 1.378O_2 + OH^-$$

The C-molar mass of such an active biomass is 24.9 kg/C-kg mol. With this equation, the theoretical value of mass conversion yields of nitrates $Y_{N/XA}$ and sulfates $Y_{S/XA}$ in biomass can be calculated:

$$Y_{N/XA} = (0.170 \text{ MM } NO_3^-)/24.9 = 0.42 \text{ kg } NO_3^-/\text{kg active biomass}$$

$$Y_{S/XA} = (0.007 \text{ MM } SO_4^{2-})/24.9 = 0.028 \text{ kg } SO_4^{2-}/\text{kg active biomass}$$

Experimental measurements of yields (Figs. 1 and 2) for nitrate and sulfate provided the values $Y_{N/XA}$ = 0.43 kg NO_3^-/kg active biomass and $Y_{S/XA}$ = 0.029 kg SO_4^{2-}/kg active biomass, respectively. These values are in fairly good agreement with the theoretical values, which validates the previous stoichiometric analysis.

Definition of Overall Absorption and Scattering Coefficients

The definition of absorption and scattering coefficients have been modified to take into account the modifications of pigment concentrations and of cell size, which occur in batch cultures during mineral limitations. Scattering must be related to the size of cells suspended in the medium and is thus proportional to the mass concentration of the total biomass C_{XT}, whereas absorption depends on pigment concentrations; absorption is thus proportional to the phycocyanin and chlorophyll content of cells, i.e., to the sum $C_{PC} + C_{CH}$.

Introducing the biotic mass fractions of phycocyanins and chlorophylls, z_{PC} and z_{CH}, a resultant biotic mass fraction of the light-harvesting antenna $z_a = z_{PC} + z_{CH}$ is calculated. Using the glycogen content of total biomass $z_G = C_G/C_{XA}$, the parameters α and δ of the light transfer model[7] can be expressed as

$$\alpha = [z_a \cdot E_a/(z_a \cdot E_a + (1 + z_G) \cdot E_s)] \quad (1)$$

$$\delta = [z_a \cdot E_a + (1 + z_G) \cdot E_S] \cdot C_{XA} \cdot \alpha \cdot L \quad (2)$$

The light transfer equations derived from Schuster's assumptions clearly depend both on the biomass concentration and on the pigment content of the cells. It is therefore justified a posteriori to describe absorption and scattering phenomena, which play different roles in light diffusion inside the reacting volume, by two parameters. These parameters, E_a and E_s, are the overall absorption and scattering mass coefficients; appropriate experimental determinations provided the following values:

$$E_a = 813 \text{ m}^2/\text{kg of antenna}$$

$$E_s = 175 \text{ m}^2/\text{kg of total biomass}$$

Kinetic Model

The biomass volumetric rate will be assumed to be calculated each time according to the following sequence, which summarizes the equations previously given.

Phycocyanin and chlorophyll concentrations C_{PC} and C_{CH} yield overall absorption coefficients; total biomass concentration C_{XT} gives overall scattering; parameters α and δ of Schuster's model provide an estimation of the available energy along the z axis $\langle 4\pi J_z \rangle$. The concept of working illuminated volume is then used to calculate the mean specific growth rate.

Two additional hypotheses should be stated now, to write the different kinetic equations for the other compounds:

1. Under mineral limitations, the mean volumetric rate of phycocyanin or protein uptake and the mean volumetric rate of biomass synthesis are both proportional to the mean linear volumetric rate of mass formation. This linear volumetric rate presents two important characteristics: (a) it is not affected by mineral limitations, which induce the synthesis of intracellular glycogen and of exopolysaccharides; (b) it remains constant during the time course of the culture, since the mean quantum yield does not change, even during mineral limitations.

2. The mean growth rate $\langle \mu \rangle$ follows a Monod law for nitrate and sulfate concentrations. In the absence of mineral limitations, the volumetric growth rate of biomass is assumed to be proportional to the phycocyanin content C_{PC} rather than to the biomass concentration. This can be justified by the fact that under light-limiting conditions, the growth metabolism is governed by the energy input rather than by enzyme activities. A biochemically structured model of the energy metabolism, including adenosine triphosphate (ATP) and reduced cofactor balances, would account for this fact more precisely.

Equation (27) of the preceding article[7] must be rewritten as follows:

$$r_x = \mu'_M \cdot C_{PC} \cdot \frac{4\pi J_z}{K_J + 4\pi J_z} \quad (3)$$

and Equation (36) from the companion article[7] becomes

$$\langle R \rangle = \langle \mu' \rangle \cdot \gamma \cdot C_{PC} \quad (4)$$

For low-energy input and assuming again that $K_J \gg F_0$,

$$r_x = \frac{\mu'_M}{K_J} \cdot 4\pi J_z \cdot z_{PC} \cdot C_{XA} \quad (5)$$

Taking the mean along the z axis provides the mean volumetric growth rate $\langle R \rangle$ for cultures not limited by minerals:

$$\langle R \rangle = \frac{\mu'_M}{K_J} \cdot z_{PC} \cdot C_{XA} \cdot \frac{F_0}{\alpha\delta} \cdot \left[1 - \frac{4\alpha + (1 - \alpha^2)(e^{\delta} - e^{-\delta})}{(1 + \alpha)^2 \cdot e^{\delta} - (1 - \alpha)^2 \cdot e^{-\delta}}\right] \quad (6)$$

Similar expressions are obtained for exponential growth and for linear light-limited growth:

$$\langle R \rangle = \frac{\mu'_M}{K_J} \cdot F_0 \cdot z_{PC} \cdot C_{XA} \quad (7)$$

$$\langle R \rangle = \frac{\mu'_M}{K_J} \cdot \frac{F_0}{E_a \cdot L} \cdot \frac{2\alpha}{1 + \alpha} \cdot \frac{z_{PC}}{z_a} \quad (8)$$

Equation (38) from the companion article,[7] which defines the working length L_2, then becomes

$$L_2 = \frac{2\alpha}{1 + \alpha} \cdot \frac{1}{z_a \cdot E_a \cdot C_{XA}} \quad (9)$$

indicating that the working length may change with the concentration of cells and with their content in light-harvesting pigments, so that

$$L_2 \div C_{XA}^{-1}$$

Using Equation (1) and provided α remains small compared with 1 leads to

$$L_2 \div z_a^{-1/2}$$

According to Equation (4) and neglecting the effects of maintenance, the mean volumetric rate for active biomass under light nitrogen or sulfur limitation is given by:

$$\langle r_{XA} \rangle = \langle R \rangle \frac{C_N}{K_N + C_N} \cdot \frac{C_s}{K_s + C_s} \tag{10}$$

where K_N and K_s are the Monod constants for nitrate and sulfate limitations, respectively.

Under N or S deprivation, the chlorophyll content of active biomass remains constant, so that the mean volumetric rate is given by

$$\langle r_{CH} \rangle = z_{CH} \cdot \langle r_{XA} \rangle \tag{11}$$

The mean volumetric rate for phycocyanins is proportional to that for active biomass in conditions of nonlimitation by minerals and to that of linear mass synthesis during N or S starvation:

$$\langle r_{PC} \rangle = z_{PC} \cdot \langle R \rangle \cdot \left[\frac{C_N}{K_N + C_N} \cdot \frac{C_s}{K_s + C_s} - \left(\frac{K_N}{K_N + C_N} + \frac{K_s}{K_s + C_s} \right) \right] \tag{12}$$

where the term on the right-hand side stands for the decrease in phycocyanin concentration, which only occurs when concentrations of nitrate and sulfate are low.

The mean volumetric rate for proteins only decreases during sulfate deprivation, so

$$\langle r_P \rangle = z_P \cdot \langle R \rangle \cdot \left[\frac{C_N}{K_N + C_N} \cdot \frac{C_s}{K_s + C_s} - q \cdot \frac{K_s}{K_s + C_s} \right] \tag{13}$$

where q is a proportionality coefficient with respect to the mean linear volumetric rate $\langle R \rangle$ and is an adjustable parameter.

The mean volumetric rate for uptake of substrates is obtained from the mass conversion yields. For nitrate and sulfate respectively,

$$\langle r_N \rangle = -Y_{N/XA} \cdot \langle r_{XA} \rangle \tag{14}$$

$$\langle r_S \rangle = -Y_{S/XA} \cdot \langle r_{XA} \rangle \tag{15}$$

The continued increase in total biomass concentration during mineral deprivation results from the accumulation of intracellular glycogen. However, if cells do not divide, growth stops when cells reach a maximum size value. This is described by the term $C_{PC}/(K_{PC} + C_{PC}^2)$, which exhibits, in addition, a Moser law in which $n = 2$. The mean volumetric rate of total biomass synthesis then is

$$\langle r_{XT} \rangle = \langle R \rangle \cdot \left[\frac{C_N}{K_N + C_N} \cdot \frac{C_s}{K_s + C_s} + \frac{C_{PC}}{K_{PC} + C_{PC}^2} \cdot \left(\frac{K_N}{K_N + C_N} + \frac{K_s}{K_s + C_s} \right) \right] \tag{16}$$

Equations (10), (12), (13), and (16) summarize the kinetic hypothesis of the model.

The mathematical model for growth of *S. platensis* in a parallelepipedic photoreactor is thus composed of Equations (4) and (10)–(16) in this article and equations (18) and (19) established elsewhere.[7] The working illuminated length has been calculated for linear growth phase assuming that the energy flux at $z = L$, F_L, should remain constant and equal to 1.0 W · m^{-2} as previously demonstrated,[7] thus leading to the transmittance ratio and to the parameter δ. The differential mathematical model can be solved with a Runge-Kutta-Merson fourth-order algorithm, the integral term being calculated at each step by a Simpson algorithm. The equations for the model are collected in Table III. This model for growth of *S. platensis* under light nitrogen or sulfur limitation uses only six parameters, μ_M', K_I, K_N, K_S, K_{PC}, and q, which remain to be identified. It must be emphasized that light absorption and diffusion parameters E_a, E_s have been measured separately.

DISCUSSION

Batch Cultures

The previous model for growth of *S. platensis* has been integrated for batch cultures performed in Roux flasks and compared with the experimental results obtained (Table I) stating the general mass balance equation:

$$\frac{dC_i}{dt} = \langle r_i \rangle$$

The six biological parameters of the model, μ_M', K_I, K_N, K_{PC}, K_s, and q, were obtained by the minimization of a quadratic criterion using a Gauss-Newton algorithm. Biomass, nitrate, sulfur, proteins, phycocyanins, and chlorophyll *a* concentrations have been taken into account. The results of the identification procedure are as follows:

$$\mu_M' = 0.52 \text{ h}^{-1}$$

$$K_I = 20 \text{ W} \cdot \text{m}^{-2}$$

$$K_N = 5.3\ 10^{-3} \text{ kg } NO_3^-/\text{m}^3$$

$$K_S = 2.5\ 10^{-4} \text{ kg } SO_4^{2-}/\text{m}^3$$

$$K_{PC} = 0.15 \text{ kg}^2 \cdot \text{m}^{-6}$$

$$q = 0.55$$

The values of μ_M' and K_I were identified from the eight experiments presented in Table I from both exponential and linear growth phases. They may be considered reliable within a confidence interval of ±5% with respect to the light transfer and physiological hypotheses that have been presented. It must be emphasized that these values represent the behavior of the culture for an incident flux varying within a factor of 5. The values of K_N, K_S, K_{PC}, and q are less precise and may vary within ±10%. Table I lists the data considered for the identification of the coefficients of the model.

Table III. Equations for the model.

$4\pi J_z$ calculation:

$$\frac{4\pi J_z}{F_0} = 2 \cdot \left[\frac{(1+\alpha) \cdot e^{-\delta(Z-1)} - (1-\alpha) \cdot e^{\delta(Z-1)}}{(1+\alpha)^2 \cdot e^{\delta} - (1-\alpha)^2 \cdot e^{-\delta}} \right]$$

$$\alpha = [z_a E_a / (z_a E_a + (1 + z_G) E_S]^{1/2}$$

$$\delta = [z_a E_a + (1 + z_G) E_S] C_{XA} \alpha L$$

Working illuminated length L_2 calculation:

$$(1+\alpha)^2 \cdot e^{\delta} - (1-\alpha)^2 - \frac{4\alpha}{T} = 0$$

$$T = F_L / F_0 \qquad F_L = 1 \text{ W} \cdot \text{m}^{-2}$$

Average of specific growth rates:

$$\langle R \rangle = \langle \mu' \rangle \cdot \gamma \cdot C_{PC}$$

$$\langle \mu' \rangle = \frac{1}{L_2} \int_0^{L_2} \mu'_M \frac{4\pi J_z}{K_I + 4\pi J_z} \cdot dz$$

Kinetic equations:

$$\langle r_{XA} \rangle = \langle R \rangle \cdot \frac{C_N}{K_N + C_N} \cdot \frac{C_S}{K_S + C_S}$$

$$\langle r_{CH} \rangle = z_{CH} \cdot \langle r_{XA} \rangle$$

$$\langle r_{PC} \rangle = z_{PC} \cdot \langle R \rangle \left[\frac{C_N}{K_N + C_N} \cdot \frac{C_S}{K_S + C_S} - \left(\frac{K_N}{K_N + C_N} + \frac{K_S}{K_S + C_S} \right) \right]$$

$$\langle r_P \rangle = z_P \cdot \langle R \rangle \left[\frac{C_N}{K_N + C_N} \cdot \frac{C_S}{K_S + C_S} - q \cdot \frac{K_S}{K_S + C_S} \right]$$

$$\langle r_N \rangle = -Y_{NXA} \cdot \langle r_{XA} \rangle$$

$$\langle r_S \rangle = -Y_{SXA} \cdot \langle r_{XA} \rangle$$

$$\langle r_{XT} \rangle = \langle R \rangle \left[\frac{C_N}{K_N + C_N} \cdot \frac{C_S}{K_S + C_S} + \frac{C_{PC}}{K_{PC} + C_{PC}} \left(\frac{K_N}{K_N + C_N} + \frac{K_S}{K_S + C_S} \right) \right]$$

Solid lines in Figures 1 and 2 show that numerical simulations are in good agreement with experimental results, therefore confirming the ability of the model to provide satisfactory predictions of biological kinetics in the photobioreactor until phycocyanins have totally disappeared. These kinetic parameters, identified here with a simple one-dimensional model, may be extended to more complex geometries, such as cylindrical photobioreactors, and to more complex physical models related to light limitation.

The illuminated volume represented here by the length L_2 may vary considerably during growth or when phycocyanin concentration decreases during mineral limitation. Figure 3 presents the time course of the ratio L_2/L in the case of nitrogen limitation (Fig. 1). This confirms that the light absorption coefficient has to be defined from pigment concentration. The linear mean volumetric rate in light-limited cultures implies that growth occurs at constant amount of illuminated pigments inside the bioreactor.

Although the mathematical formulation adopted in this work affords good predictions for kinetics and mass balances in the photobioreactor, energetic aspects have been neglected. In its current state, the physical part of the model does not enable the amount of radiant energy absorbed by the culture to be assessed with sufficient accuracy, thus precluding enthalpic balance on the process. However, Aiba[1] proposed calculating the amount of light energy absorbed by cells using the tridimensional form of the equation of radiative transfer. This approach then leads to a new definition of the mean growth rate in the culture, based on the assessment of energy conversion yields.

Continuous Cultures

The previous model can be used to predict the behavior of continuous cultures. At steady state, the mass balances are written as

$$DC_{i0} - DC_i + \langle r_i \rangle = 0$$

where C_{i0} is a concentration in the influent. Subscript i denotes biomass or biomass fractions. $C_{i0} = 0$. From experimental and/or model values of $\langle r_{xi} \rangle$ and of C_{xi} the values of the dilution rate D can be calculated according to the previous mass balance. The biomass productivity in the bioreactor is given by DC_{XA}. Such calculations were performed in different experimental conditions

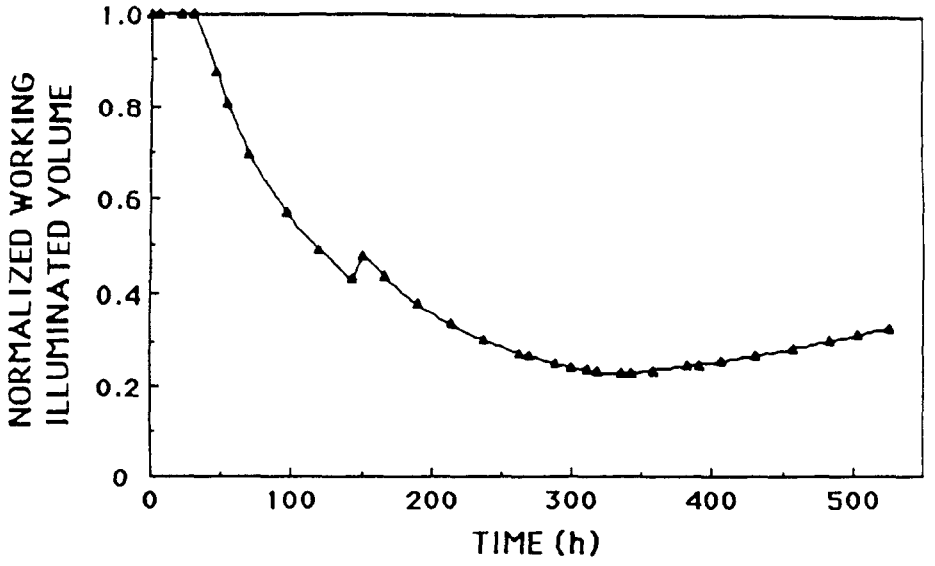

Figure 3. Time course of the working illuminated volume during batch culture of *S. platensis* in photobioreactor under NO_3^- depletion; F_0 is 8 W · m^{-2} before 144 h and 12 W · m^{-2} after.

and are reported in Figure 4, where productivity is plotted versus dilution rate.

Figure 4 shows that in the case of light limitation alone and for a fixed energy flux (20 W · m^{-2}) the productivity profile is flat between 0.005 and 0.022 h^{-1} for D. The optimal dilution rate (with respect to productivity) may be chosen in a wide range of D. This is because the amount of illuminated phycocyanins remains constant in these conditions, in spite of changes in the working illuminated volume that result from changes in phycocyanin concentrations, themselves defined by the chosen dilution rate. Conversely, when the process is governed by mineral limitation, the biomass productivity displays a classical optimum at a fixed value of D. When both light energy and mineral limitations occur, intermediate behavior may be observed (Fig. 4). These results indicate that it is necessary to represent a continuous culture to account for pigment intracellular concentrations and for working illuminated volume changes.

The robustness of the model and its ability to predict stationary behavior of the culture in the photobioreactor depend on both the accuracy of the kinetic parameters used and of the physical light transfer hypotheses. The kinetic parameters are easily determined using the concept of working illuminated volume. It must be pointed out that a simpler light transfer model (Beer-Lambert's

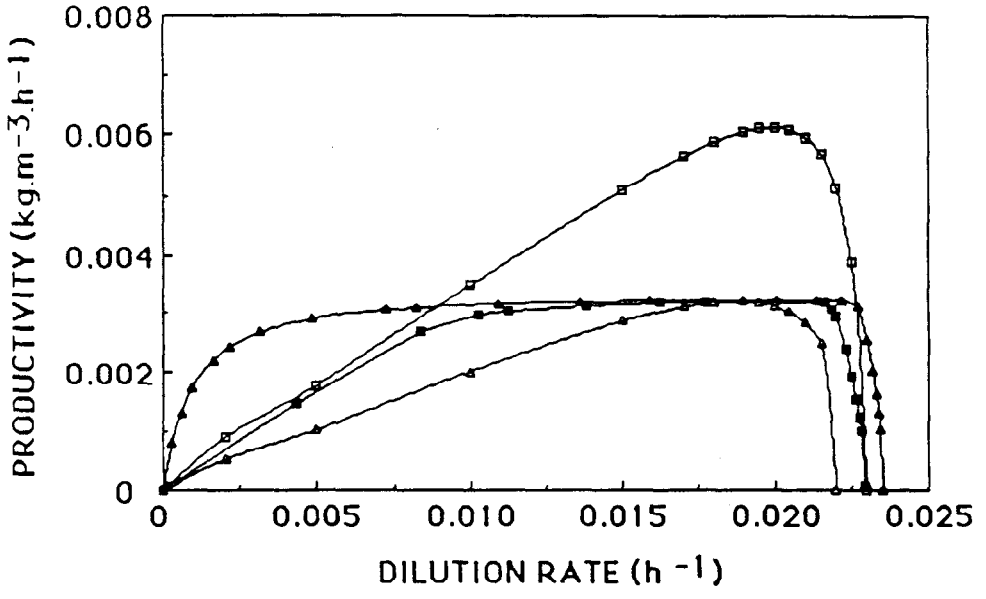

Figure 4. Effects of mineral (NO_3^-) and light limitations on the productivity of a continuous culture of *S. platensis* in photobioreactor (F_0 = 20 W · m^{-2}): (□) nitrate limitation (input concentration C_{NiO} = 0.16 kg · m^{-3}); (▲) light limitation; (■) nitrate and light limitation (input concentration C_{NiO} = 0.16 kg · m^{-3}); (△) nitrate limitation (input concentration C_{NiO} = 0.093 kg · m^{-3}).

model) would not be able to represent experimental results in such a large domain of incident light flux and different substrate concentrations either in batch or in steady-state conditions.

CONCLUSION

Physical modeling of photosensitized reactions raises the problem of light limitation. This is a typical dimensional problem, which has to be taken into account and rationalized for determination of kinetic parameters. For this purpose, a vessel of simple, monodimensional geometry may be used to define a working illuminated volume. The values of kinetic parameters obtained in this way can then be extended to more complex geometries such as cylindrical photobioreactors.

In such tridimensional conditions, determination of kinetic and energy parameters (energetic mass conversion yields and enthalpic balances) requires the radiant energy absorbed by the culture to be known, which can be achieved by solving the tridimensional form of the equation of radiative transfer given the local specific intensity.

Finally, biochemically structured models[12] would more accurately predict the metabolic deviations in microorganisms submitted to environmental stresses, and they also would allow the number of identified parameters required for the model to be reduced.

ACKNOWLEDGMENTS

This work was supported by the Centre National d'Etudes Spatiales and by the European Space Agency.

NOMENCLATURE

C_i	concentration of compound i ($kg \cdot m^{-3}$)
D	dilution rate (h^{-1})
E_a	global absorption mass coefficient ($m^2 \cdot kg^{-1}$)
E_i	global scattering mass coefficient ($m^2 \cdot kg^{-1}$)
F	radiant energy flux ($W \cdot m^{-2}$)
J	mean light intensity ($W \cdot m^{-2}$)
K_J	half saturation constant for radiant energy available ($W \cdot m^{-2}$)
K_N	half saturation constant for nitrate concentration ($kg \cdot m^{-3}$)
K_{PC}	half saturation constant for phycocyanin concentration ($kg^2 \cdot m^{-6}$)
K_S	half saturation constant for sulfate concentration ($kg \cdot m^{-3}$)
L	length of bioreactor (m)
L_2	length of illuminated volume (m)
MM	molar mass ($kg \cdot kmol^{-1}$)
PS	photosystem
q	coefficient of proportionality (dimensionless)
r_i, R	volumetric rate of compound i ($kg \cdot m^{-3} \cdot h^{-1}$)
Y	mass conversion yield (dimensionless)
z_i	mass biotic fraction of compound i (dimensionless)
$\langle\rangle$	mean volumetric integral, $= \frac{1}{V} \iiint_V \cdot dV$

Greek letters

γ	illuminated fraction of bioreactor volume (dimensionless)
μ	growth rate (h^{-1})
μ_M, μ'_M	maximum growth rate (h^{-1})

Subscripts

a	antenna compound
CH	chlorophyll *a* compound
G	glycogen compound
N	nitrate compound
P	protein compound
PC	phycocyanin compound
S	sulfate compound
X	biomass compound
XA	active biomass compound
XT	total biomass compound

References

1. Aiba, S. 1982. Growth kinetics of photosynthetic microorganisms. *Adv. Biochem. Eng.* **23**: 85–156.
2. Allen, M. M., Hutchison, F. 1980. Nitrogen limitation and recovery in the cyanobacterium *Aphanocapsa* 6308. Arch. Microbiol. **128**: 1–7.
3. Allen, M. M., Law, A., Evans, E. H. 1990. Control of photosynthesis during nitrogen depletion and recovery in a non-nitrogen-fixing cyanobacterium. Arch. Microbiol. **153**: 428–431.
4. Allen, M. M., Smith, A. J. 1969. Nitrogen chlorosis in blue green algae. Arch. Mikrobiol. **69**: 114–120.
5. Bennet, A., Bogorad, L. 1973. Complementary chromatic adaptation in a filamentous blue-green alga. J. Cell Biol. **58**: 419–435.
6. Cawse, P. A. 1967. The determination of nitrate in soil solutions by U.V. spectrophotometry. Analyst **92**: 311–315.
7. Cornet, J. F., Dussap, C. G., Dubertret, G. 1992. A structured model for simulation of cultures of cyanobacterium *Spirulina platensis* in photobioreactors: I. Coupling between light transfer and growth kinetic. Biotechnol. Bioeng.
8. Herbert, D., Phillips, P. J., Strange, R. E. 1971. Chemical analysis of microbial cells. Meth. Microbiol. **5b**: 209–394.
9. Lehman, M., Wober, G. 1976. Accumulation mobilisation and turnover of glycogen in the blue-green bacterium *Anacystis nidulans*. Arch. Microbiol. **111**: 93–97.
10. Myers, J., Kratz, K. A. 1955. Relation between pigment content and photosynthetic characteristics in blue green alga. J. Gen. Physiol. **39**: 11–22.
11. Peschek, G. A. 1987. Respiratory electron transport. pp. 118–150. In: P. Fay and C. Van Baalen (eds.): The cyanobacteria. Elsevier, Amsterdam.
12. Roels, J. A. 1983. Energetics and kinetics in biotechnology. Elsevier Biomedical, New York.
13. Terho, T.T., Hartiala, K. 1971. Method for determination of the sulfate content of glucosaminoglycans. Anal. Biochem. **41**: 417–476.
14. Yamanaka, G., Glazer, A. N. 1980. Dynamic aspects of phycobilisome structure. Phycobilisome turnover during nitrogen starvation in *Synechococcus* sp. Arch. Microbiol. **124**: 39–47.
15. Zarrouk, C. 1966. Contribution à l'étude d'une cyanophycée. Influence de divers facteurs physiques et chimiques sur la croissance et la photosynthèse de *Spirulina maxima* Geitler. Ph.D. Thesis, Université de Paris.

ERRATA.

MODELING OF PHYSICAL LIMITATIONS IN PHOTOBIOREACTORS.

TN.19.1: Adaptation of the light energy transfer model to cylindrical geometries.

- In TN.19.1, the definitions of parameters α and δ are ambiguous when mineral limitations occur, and in order to avoid any confusion, the definitions should become:

$$\alpha = \left[Ea(C_{PC} + C_{CH})/\left[Ea(C_{PC} + C_{CH}) + EsC_{XT}\right]\right]^{1/2}$$

$$\delta = \left[Ea(C_{PC} + C_{CH})\left[Ea(C_{PC} + C_{CH}) + EsC_{XT}\right]\right]^{1/2} R$$

- The definition of average of specific growth rates in cylindrical coordinates $<\mu'>$ are mistaken and should be:

$$<\mu'> = \frac{1}{\pi R_2'^2}\int_0^{R_2'} 2\pi r \mu_M' \frac{4\pi J_r}{K_J + 4\pi J_r} dr + \frac{1}{\pi\left(R^2 - R_2^2\right)}\int_{R_2}^{R} 2\pi r \mu_M' \frac{4\pi J_r}{K_J + 4\pi J_r} dr$$

or

$$<\mu'> \approx \frac{1}{\pi\left(R^2 - R_2^2\right)}\int_{R_2}^{R} 2\pi r \mu_M' \frac{4\pi J_r}{K_J + 4\pi J_r} dr$$

In the same way, the definition of γ should be:

$$\gamma = \frac{R_2'^2}{R^2} + \frac{\left(R^2 - R_2^2\right)}{R^2}$$

and $<R> = <\mu'> \gamma C_{PC}$.